TAMPEREEN TEKNILLINEN YLIOPISTO
TAMPERE UNIVERSITY OF TECHNOLOGY

LUTFI SAMARA

PHASE NOISE ESTIMATION AND MITIGATION IN UPLINK OFDMA

Master of Science Thesis

Examiners: Prof. Mikko Valkama and Dr. Ville Syrjälä.
Examiner and topic approved in the Faculty of Faculty of Computing and Electrical Engineering council meeting on 08 November 2013

ABSTRACT

TAMPERE UNIVERSITY OF TECHNOLOGY
Master's Degree Program in Information Technology
Samara, Lutfi: Phase Noise Estimation and Mitigation in Uplink OFDMA
Master of Science Thesis: 46 Pages
October 2013
Major: Communications Engineering
Examiners: Prof. Mikko Valkama and Dr. Ville Syrjälä
Keywords: Phase Noise, OFDM, OFDMA, Uplink OFDMA, Estimation, Mitigation, Inter-Carrier Interference, Inter-User Interference.

Orthogonal Frequency Division Multiplexing (OFDM) and Orthogonal Frequency Division Multiple Access (OFDMA) are modulation techniques that are deployed in various communications standards in today's communication technology. The reason for their selection is the multitude of advantages that they offer over other modulation techniques that meet the increasing demands on high data rate communications. Consequently, this necessitates the need to devise mitigation methods for various impairments that accompany the implementation of OFDM and OFDMA.

This thesis focuses on the oscillator phase noise and its mitigation in uplink OFDMA systems to achieve a better overall system performance in terms of transceiver Bit-Error-Rate (BER). In OFDMA systems, the unequal uplink power levels of each user acts as a catalyst for the phase noise induced spreading effect that users with a higher power have on users with a lower one. This spreading effect is named Inter-User Interference (IUI). The simulation results depict the performance of various phase noise mitigation methods as a function of different received powers and phase noise levels in the uplink case for a user in an OFDMA symbol. The devised IUI mitigation method achieves a significant gain over the conventional methods of phase noise mitigation which do not take into account the effect of the IUI.

PREFACE

There are a number of people to whom I am greatly indebted since without them, this journey of studies and work might not have been possible.

First off, I would like to express the deepest appreciation to my supervisors and examiners, Prof. Mikko Valkama and Dr. Ville Syrjälä for their invaluable aid. Without their guidance and persistent help, this thesis work would not have been possible.

I would like to thank my family for their encouragement and support throughout the course of my studies in Tampere, Finland. I know I have put you through a lot of stress to pursue the completion of my studies and I hope it was worth it.

I would also like to place on record my sincere gratitude to Dr. Ridha Hamila for his suggestion and encouragement to join the Electronics and Communications Engineering department at Tampere University of Technology.

Finally, I hope that this work genuinely projects the efforts that I have spent in order to complete it in the best possible form, and I hope it will be my gateway to a more fruitful future.

Tampere, 8th of October 2013

Lutfi Samara

Contents

LIST OF ABBERVIATIONS

3GPP	3rd Generation Partnership Project
ADC	Analog-to-Digital Converter
AF	Amplify-and-Forward
AWGN	Additive White Guassian Noise
BER	Bit Error Rate
BPSK	Binary Phase Shift Keying
CDMA	Code Division Multiple Access
CP	Cyclic Prefix
CPE	Common Phase Error
DC	Direct Current
DFT	Discrete Fourier Transform
DL	Downlink
DSSS	Direct-Sequence Spread Spectrum
DVB-T	Digital Video Broadcasting - Terrestrial
EVM	Error Vector Magnitude
FDMA	Frequency Division Multiple Access
FFT	Fast Fourier Transform
FRO	Free-Running Oscillator
GI	Guard Interval
GSM	Groupe Spécial Mobile
HSPA	High-Speed Packet Access
I/Q	In-Phase / Quadrature-Phase
ICI	Inter-Carrier Interference
IDFT	Inverse Discrete Fourier Transform
IEEE	Institute of Electrical and Electronics Engineers
IFFT	Inverse Fast Fourier Transform
IP	Internet Protocol
ISI	Inter-Symbol Interference
ITU-R	International Telecommunication Union - Radiocommunication Sector
IUI	Inter-User Interference
LI-CPE	Linear Interpolation - Common Phase Error
LI-TE	Linear Interpolation - Tail Estimation
LPF	Low Pass Filter
LS	Least Squares
LTE	Long Term Evolution
LTE-A	Long Term Evolution - Advanced
MIMO	Multiple-Input and Multiple-Output
MPEG	Moving Picture Experts Group
MS	Mobile Station

OFDM	Orthogonal Frequency Division Multiplexing
OFDMA	Orthogonal Frequency Division Multiple Access
PAPR	Peak-to-Average Power Ratio
PN	Phase Noise
PSD	Power Spectral Density
QAM	Quadrature Amplitude Modulation
QPSK	Quadrature Phase Shift Keying
RF	Radio Frequency
SC-FDMA	Single-Carrier Frequency Division Multiple Access
SNR	Signal-to-Noise Ratio
TPS	Transmission Parameter Signalling
UL	Uplink
UMTS	Universal Mobile Telecommunications System
Wi-Fi	Wireless Fidelity
Wi-MAX	Worldwide Interoperability for Microwave Access
WLAN	Wireless Local Area Network

1. INTRODUCTION

1.1. Background and Motivation

Long Term Evolution (LTE), Wireless Local Area Network (WLAN) and Digital Video Broadcasting - Terrestrial (DVB-T), are all examples of communications standards that deploy multicarrier modulation as a digital data transmission technique. Orthogonal Frequency Division Multiplexing (OFDM) is the most widely implemented multicarrier modulation technique. Its high spectral efficiency, robust performance in frequency selective channels and efficient implementation using the Fast Fourier Transform (FFT) algorithm are some of the many advantages that qualify it to be selected for high data rate transmission [11]. However, these compelling advantages are not free of side effects that accompany the implementation of OFDM. Some of these disadvantages are high Peak-to-Average-Power Ratio (PAPR), loss of efficiency due to the deployment of a Guard Interval (GI) and sensitivity to frequency errors [21].

Oscillator phase noise is one of the frequency errors that the OFDM technique is sensitive to. Phase noise is a term that refers to the non-stable phase of the oscillating signal in up and down-converting oscillators in a transceiver leading to interference between subcarriers in OFDM. This phenomenon is referred to as Inter-Carrier Interference (ICI) which will eventually cause an overall performance degradation of the communication system performance. However, the performance degradation is not solely confined to ICI, but Inter-User Interference (IUI) surpasses this in-band effect in some scenarios. Many phase noise compensation techniques have been studied to combat the in-band ICI effect [27], [29], [30], [31], [32] and some of these compensation techniques will be deployed in the phase noise induced out-of-band spread mitigation in uplink OFDMA systems.

1.2. Contribution of the Thesis

This thesis addresses the phase noise induced out-of-band interference in an OFDM multiple access technique, which is referred to as Orthogonal Frequency Division Multiple Access (OFDMA), where the subcarriers are contiguously assigned for each

user while each user suffers from the phase noise effect in the uplink stage. Accompanied by a difference in each user's power level at the Base Station (BS) receiver, this leads to out-of-band interference between the users in an OFDMA symbol, or more practically called Inter-User Interference (IUI). A mitigation method is devised to improve the overall system performance characterized by the Bit-Error-Rate (BER) of the system.

1.3. General Outline

This thesis is structured as follows. After the introduction, Chapter 2 addresses the theoretical background of OFDM and OFDMA, the challenges faced in this modulation technique and a quick overview of some of the wireless communication standards that use OFDM and OFDMA as a way for data transmission. Next, Chapter 3 investigates the phase noise model along with its effect on a general I/Q and OFDM signals. Subsequently, Chapter 4 provides several phase noise mitigation techniques in OFDM systems as well as the modeling of the effect of phase noise in uplink OFDMA, and ending with the development of a compensation technique for phase noise induced interference in uplink OFDMA. Subsequently, in Chapter 5, simulation parameters that were used in this thesis along with the results of the proposed phase noise compensation technique in OFDMA systems are presented. Lastly, in the final chapter, a conclusion and future work suggestions are presented based on the results.

2. OFDM AND OFDMA BACKGROUND

In this chapter, a theoretical review of the structure and operation of a general OFDM system is presented. Next, multiple user access in OFDM, OFDMA, is presented while highlighting the pros and cons of using this multiple access technique. Subsequently, the next section will shed light on practical limitations from an implementation point of view where it acts as a good introduction for the next chapter. Finally, the last section sheds some light on the diverse applications of OFDM and OFDMA in various standards of data communications like LTE, WLAN and DVB-T.

2.1. Basics of OFDM

OFDM is a special form of multicarrier modulation where the data is transmitted by dividing the input subcarrier stream into symbols so that each symbol contains several orthogonal subcarriers. This multicarrier modulation technique is attractive and widely implemented since it shows robustness against hostile frequency selective fading channels and thus making it adequate for high speed data transmission [11]. This is done by having the individual bandwidth of a subcarrier within the OFDM symbol less than the coherence bandwidth of the channel which causes a flat fading effect from a single subcarrier point of view. The channel can be equalized using a trivial frequency domain single tap equalizer [21].

The OFDM subcarriers are organized in such a manner that they overlap in the frequency domain while orthogonality is still ensured to be able to separate them from each other at the receiver front end. The overlapping frequency domain subcarriers provide better spectral efficiency than that of Frequency Division Multiple-Access (FDMA) systems, where no spectral overlap of the subcarriers is allowed [11]. Figure 2.1 depicts the spectra of three subcarriers within an OFDM symbol.

As it can be seen from in Figure 2.1, each peak of each OFDM subcarrier coincides with the zero crossings of the other subcarriers therefore fulfilling the orthogonality requirement of an OFDM system.

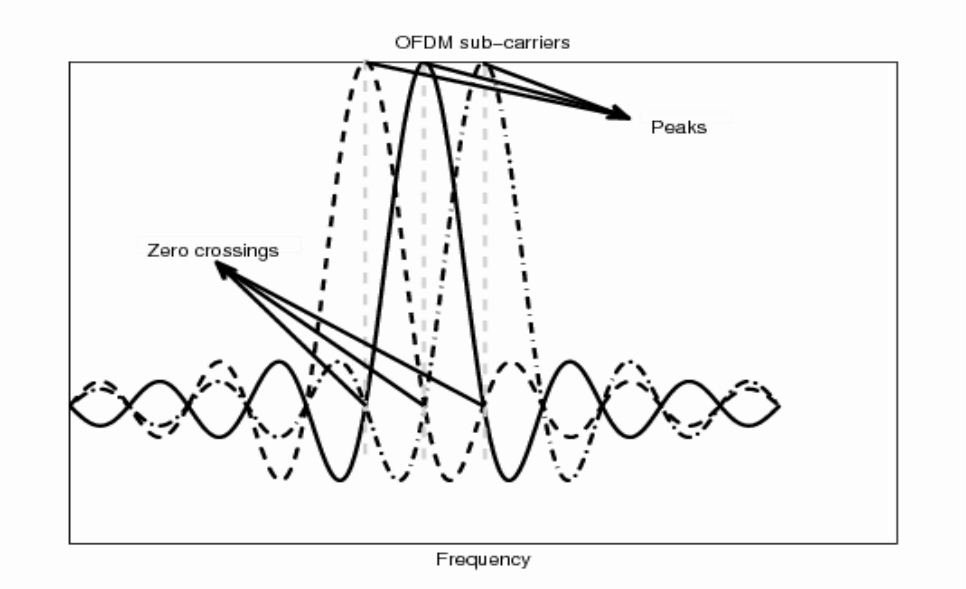

Figure 2.1 *- The spectrum of an OFDM symbol which consists of several subcarriers*

Other factors which justify the preference of using multicarrier modulations are the maturity that this modulation type gained over the years of research and the synergetic effect that results when OFDM and Code Division Multiple Access (CDMA) are combined [20].

The implementation of the orthogonality between *N* subcarriers is achieved by applying the inverse discrete Fourier transform to subcarrier modulated symbols, which yields

$$x_n(m) = \frac{1}{\sqrt{N}} \sum_{k=0}^{N-1} X_k(m) e^{j2\pi kn/N}, \tag{2.1}$$

where $x_n(m)$ is the *m*th transmitted OFDM symbol, $X_k(m)$ is a subcarrier modulated symbol belonging to the *m*th transmitted OFDM symbol, and $n \in [0, N-1]$. If the sampling time is denoted by T_s and the sampling frequency is $F_s = 1/T_s$, the subcarrier spacing will be represented by $1/(NT_s)$. The symbol duration of an OFDM symbol is NT_s.The processing of (2.1) is applied by performing an Inverse Discrete Fourier transform (IDFT) function which is efficiently computed using the Inverse Fast Fourier Transform Algorithm (IFFT). In the reception, the received signal undergoes a Fast Fourier Transform (FFT) operation to undo the IFFT process applied at the transmission stage.

The next step in an OFDM system is the insertion of a guard interval. The Guard Interval (GI) is inserted in the time domain, after the IFFT operation, to insure that the received OFDM symbol does not suffer from Inter-Symbol Interference (ISI). ISI is caused by the delay spread of a frequency selective channel. The cyclic prefix time T_{cp} should be greater than the maximum delay spread of the channel denoted by τ_{max} for perfect immunity to ISI. After the addition of the GI, the OFDM symbol duration will be longer and is written as $(N+G)T_s$ seconds, where G here represents the guard length in samples. Figure 2.2 shows how the last part of the OFDM symbol is copied and added to its beginning.

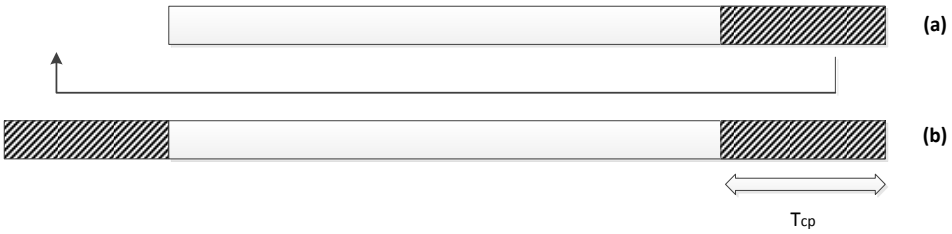

Figure 2.2 *- (a) No cyclic prefix inserted and (b) cyclic prefix inserted*

After the signal is up-converted and transmitted, it passes through the time-invariant channel and Additive White Gaussian Noise (AWGN) will be added. At the receiver front end, the received signal will be down-converted and the guard interval will be removed. The *mth* received symbol can be written as

$$\mathbf{r}_m = (\mathbf{h}_m * \mathbf{x}_m) + \mathbf{z}_m \,, \tag{2.2}$$

where $\mathbf{h}_{\mathrm{m}}$ is the ($D \times 1$) multipath channel impulse response where D should be less than the G, $\mathbf{x}_{\mathrm{m}} = [x_0(m), x_1(m), x_2(m), \dots, x_{N-1}(m)]^T$, $\mathbf{z}_{\mathrm{m}}$ is ($N \times 1$) vector that denotes the Additive Whit Gaussian Noise (AWGN) and the operator " $*$ " denotes a circular convolution operation. The previous equation can be simplified using the circulant convolution matrix [15], so the simplified equation is:

$$\mathbf{r}_m = \mathbf{H}_m \mathbf{x}_m + \mathbf{z}_m \,, \tag{2.3}$$

where $\mathbf{H}_m$ is the circulant convolution matrix related to the channel impulse response $\mathbf{h}_m$.

The signal is finally received after it passes through the channel to be detected using Fast Fourier Transform (FFT) processing, and the signal can be written as

$$r_n(m) = \frac{1}{\sqrt{N}} \sum_{k=0}^{N-1} R_k(m) e^{-j2\pi kn/N}, \quad (2.4)$$

where $R_k(m)$ is the received OFDM signal containing the channel effect and the AWGN.

At this stage, it is necessary to estimate the channel effect in order to mitigate it. There exist various ways of implementing channel estimation methods, however, in OFDM, a novel technique was developed to achieve this purpose. This technique involves the insertion of reference data within an OFDM symbol which is referred to as pilot data. The pilot data are subcarriers that are known to the receiver and used to estimate the channel effect. The pilot data can be also used to estimate other unwanted effects that are in the received OFDM signal. For instance, it could be used in e.g. OFDM symbols synchronization or in phase noise estimation. There are many configurations for the insertion of the pilot subcarriers within an OFDM symbol depending on the standard in use. For instance, LTE and DVB-T have different pilot subcarrier configuration within an OFDM symbol. The pilots are distributed uniformly throughout the time and frequency axes in order to detect both the varying time and frequency unwanted effects that affect and OFDM symbol. Figure 2.3 shows an example of a distribution of pilot subcarriers in several OFDM symbols. The distribution of pilot data in this illustration is a simple equally spaced pilot data, and all OFDM symbols have similar pilot subcarrier distribution, however, this is not the case in most of the wireless communications standards. The dark circles that represent the pilot subcarriers in Figure 2.3 are picked up at the receiver stage and used to estimate the channel frequency response or any other effect that needs to be estimated. A block diagram reviewing the sequence of operations in an OFDM transmission and reception is shown in Figure 2.4.

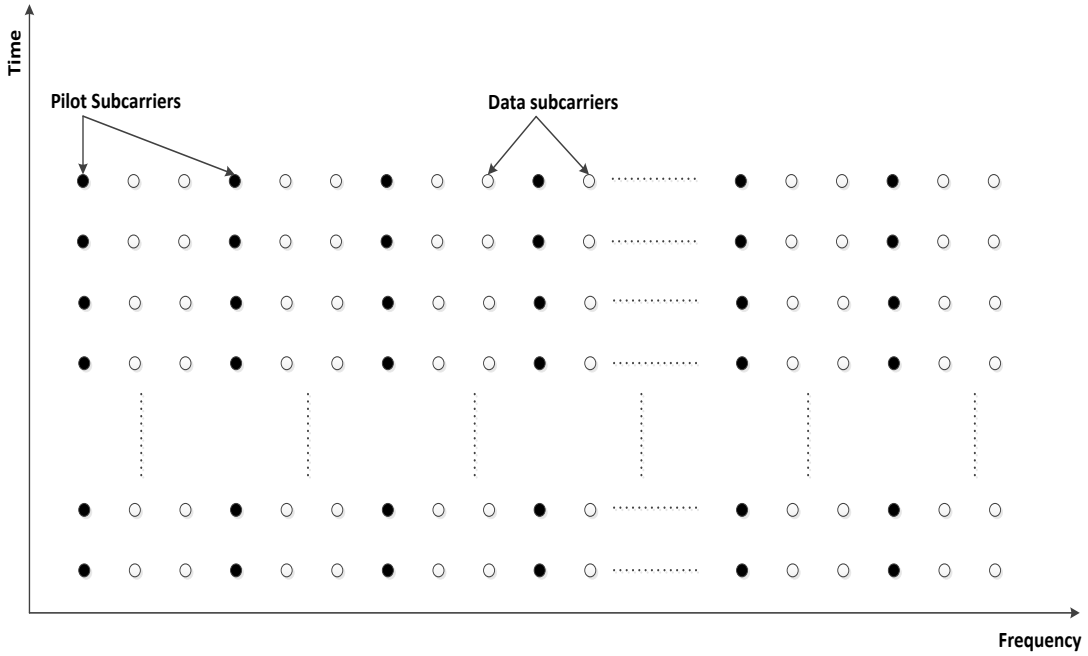

Figure 2.3 *- Equally spaced pilot subcarriers in OFDM symbols*

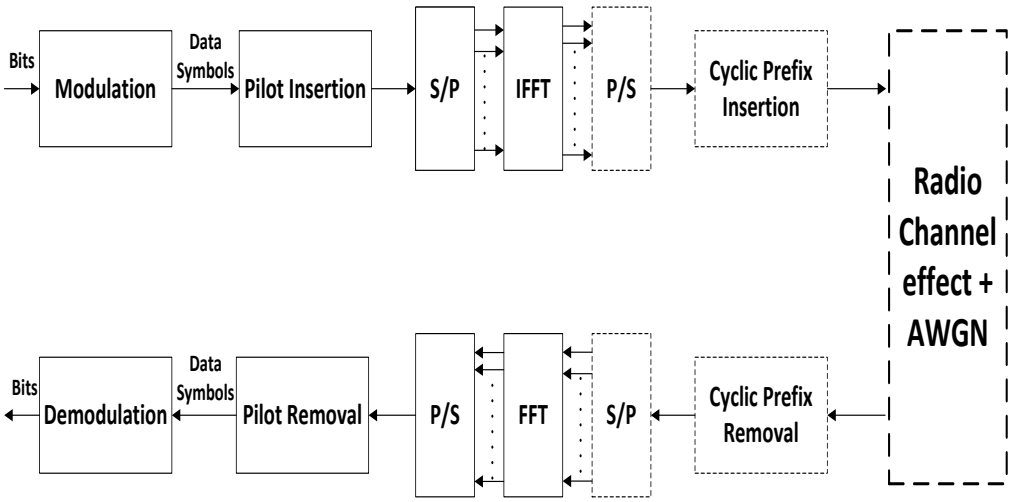

Figure 2.4 *- OFDM baseband transmission and reception chain. The un-dashed blocks represent the operations happening in the frequency domain while the dashed ones represent the operations happening in the time domain.*

2.2. Basics of OFDMA

OFDMA is a modulation technique that uses the same concepts as in OFDM except that it has the extra feature of assigning multiple users at the same time. This is done by assigning different subcarriers for different users instead of assigning all the subcarriers in the OFDM symbol to a single user. In an OFDM system, different users need to wait

a certain amount of time in turns. In OFDMA, instead of having full OFDM symbols at a certain time for each user, users simultaneously access the channel through different assigned subcarriers.

In OFDMA, there exist two ways to assign subcarriers to different users. They are distributed and contiguous [36]. In a distributed subcarrier assignment, the users' subcarriers are spread in the OFDM symbol in a pseudorandom fashion while in the contiguous case; the subcarriers are assigned to each user in contiguous chunks [36]. Besides the advantages of OFDM that are included in OFDMA, OFDMA offers a couple of important advantages depending on the assignment of the subcarriers. In the case of the distributed subcarriers case, OFDMA offers a frequency diversity advantage since the subcarriers experience different channel effects when they are distributed throughout the whole symbol. Additionally, in both of the subcarriers assignment cases, a multiuser diversity occurs because of the different channels that each user experiences since each user will be located in a different environment [36]. Figure 2.5 shows the different assignment methods that are discussed above.

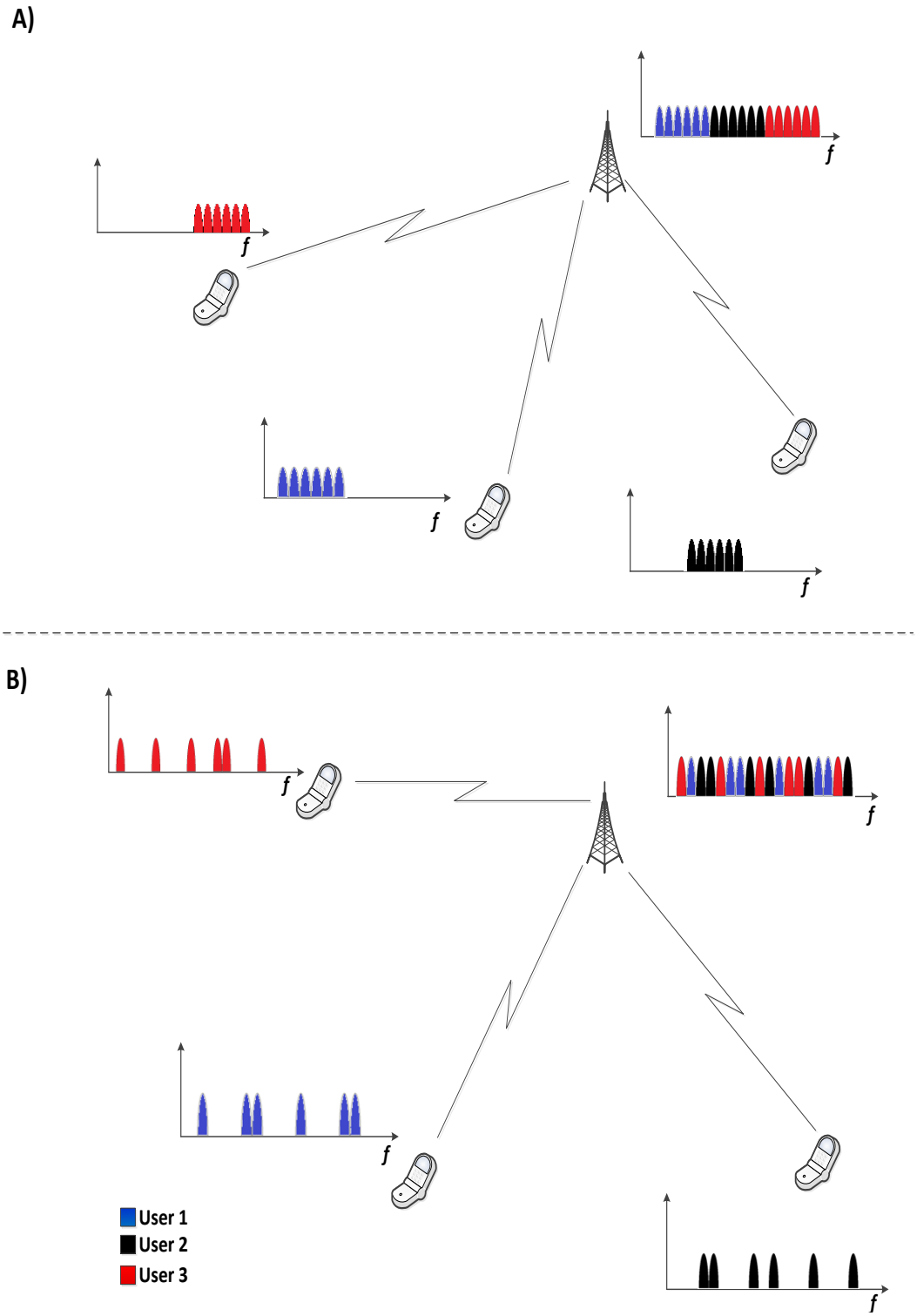

Figure 2.5 *– Different subcarriers assignment in uplink OFDMA. A) Contiguous assignment and B) distributed assignment.*

One important issue to consider in an OFDMA transmission scheme is the transmission-timing control. It is necessary to have an approximately identical reception time for the signals of all mobile terminals at the base station. The transmissions from different mobile terminals should be received at the base station with a timing

misalignment that is less than the length of the cyclic prefix to preserve the orthogonality between the subcarriers received from the different mobiles and thus avoid inter-user interference [36].

Furthermore, due to the variations in the distances between each mobile terminal and the base station, this will lead to variations in the propagation delay where the propagation delay time exceeds the cyclic prefix time T_{cp} in some cases. This necessitates an uplink transmission-timing control for each mobile terminal [36]. The transmit-timing control adjusts the transmission time of each mobile terminal in the cell to guarantee an approximate timing alignment of the received signals at the base station [36]. In addition, due to the expected continuous movement of mobile terminals within a cell, the transmit-timing control should be continuously active in order to align the received signals from the different mobile terminals at the base station [36].

Another issue related to the different distances of the mobile terminals from the base station is the transmit-power control. In OFDMA, all users will share the same OFDM symbol as discussed previously and depicted in Figure 2.5. This leads to a difference between the received powers at the base station due to the fact that each mobile terminal experiences a different path loss. When there is a significant power difference between the transmitting mobile stations, the impact of frequency errors is severe and will degrade the efficiency of data transmission in an OFDMA symbol. These frequency errors that affect the subcarriers of a user that possesses higher power in the OFDMA symbol will spread its effect on the neighboring subcarriers that belong to other users. This leads to the loss of orthogonality between the different subcarriers. To avoid this situation, an uplink transmit-power control needs to be applied in the case of uplink OFDMA, which reduces the power differences between the users and ensure that the received signals at the base station are approximately at the same power level [36]. In case the uplink transmit-power control is not working perfectly, compensations at the receiver should be applied to boost up the system performance.

2.3. OFDM and OFDMA Imperfections

The tempting advantages of spectral efficiency and modulation ease in OFDM, as previously presented, are accompanied with some disadvantages. A receiver in a communication system should be able detect the received data whatever is transmitted.

The detection should take into account the phase, time and frequency of the transmitted signal. The environment that a receiver operates in affects the received signal, and the receiver should take these environmental effects into account. An additional issue to consider here are the impairments in an OFDM transceiver that are caused by many factors and briefly discussed in the following sections.

2.3.1. Frequency Offset

The frequency offset phenomenon in OFDM systems is caused by two factors: a mismatch between the transmitter and receiver sampling clocks, and the misalignment between the reference frequency of the transmitter and the receiver [21]. The sampling clock mismatch between the transmitter and the receiver is due to the fact that the sampling epoch in the receiver Analog-to-Digital Converter (ADC) is rarely matching the one in the transmitter causing the receiver sampling to slowly drift from the transmitter [21]. The effect of the sampling clock mismatch and carrier frequency offset are manifested in two ways [21]: Rotation of the subcarriers due to the slow variation in the sampling time instant which will cause a reduction of the Signal-to-Noise Ratio (SNR) due to ICI, and loss of orthogonality due to the energy spread of subcarriers.

2.3.2. Timing Offset

Timing synchronization between the transmitter and the receiver is essential to maintain a connection where the OFDM symbols are correctly detected and decoded. The timing synchronization is possible to achieve with the introduction of training sequences in addition to the data symbols in an OFDM system [21]. The receiver may not be able to completely synchronize the received symbols with the transmitted ones due to the channel impairments. The timing offset is manifested in the system by causing a phase rotation of the subcarriers [21]. The timing offset can be avoided by e.g. the use of a cyclic prefix as indicated previously.

2.3.3. Power Amplifier Nonlinearity

Power Amplifier (PA) nonlinearity is a major system impairment in an OFDM system due to the OFDM waveform’s large dynamic range with respect to its power [12]. The large dynamic range in an OFDM signal related to its power is characterized by a high Peak-to-Average Power Ratio (PAPR). This impairment is manifested by a nonlinear distortion added to the OFDM signal when it passes through a nonlinear PA which causes serious in-band distortion as well as adjacent channel interference due to the

spectral regrowth in the transmitted signal [12]. Many PAPR reduction methods have been proposed to improve the performance of the OFDM transmission by improving the bit-error rate performance and, additionally, allowing the use of a low-power hardware which means reducing the electricity costs and increasing battery life [33].

2.3.4. Oscillator Phase Noise

The arrangement of subcarriers in a way that they overlap in the frequency domain introduces high sensitivity to frequency errors. Each peak of a single subcarrier should align perfectly with the zero crossings of the other subcarriers in the OFDM symbol; otherwise, this would cause what is known as Inter Carrier Interference (ICI). One of the causes of ICI is caused by, i.e., phase noise in the transmitter and receiver oscillators [21]. Such phase rotation is caused by non-stable phase of the oscillating signal at up and down conversions at the transceiver [21].

ICI is combated using subcarriers that are known a priori to the receiver. These subcarriers are used to estimate the phase noise and compensate it at later stages in the OFDM receiver. The next chapters will thoroughly discuss this issue.

2.4. Applications of OFDM and OFDMA

The mobile wireless systems are evolving to cope up with the increasing demand for higher throughput figures. The previous mobile wireless communications technologies such as UMTS adopted the Direct-Sequence Spread Spectrum (DSSS) modulation technique , while later systems like LTE, Long Term Evolution – Advanced (LTE-A), Worldwide Interoperability for Microwave Access (WiMax), WLAN and DVB-T all shifted to OFDM and OFDMA [11]. The reason for such a shift is that OFDM offers several advantages in delivering high-speed data in a multipath, frequency selective fading environments [11]. In this subsection, several current communication technologies that implement a multicarrier modulation technique are briefly presented. This is done to give the reader a sense of coherence on the importance of the overall enhancement of the performance of multicarrier techniques such as OFDM and OFDMA that are deployed in modern day communication technologies.

2.4.1. Long-Term Evolution (LTE)

Developed by the 3rd Generation Partnership Project (3GPP), LTE is a standard for high-speed data communication for mobile phones and data terminals. It was suggested

and developed to increase the capacity and speed by using a different radio interface and core network improvements when compared with previous standards of wireless communications like the GSM and UMTS [17]. LTE uses OFMDA and Single-Carrier Frequency-Division Multiple Access (SC-FDMA) in its downlink and uplink respectively.

The LTE design targets concerning its capabilities as documented in 3GPP TR 25.91 [2] specify that the downlink and uplink peak data-rate are 100 Mbits/s and 50 Mbits/s respectively , when operating in a 20 MHz bandwidth [13]. This means that the requirements can be expressed as 5 bits/s/Hz for the downlink and 2.5 bits/s/Hz for the uplink case. In addition, LTE should be able to support at least 200 mobile terminals when operating at 5 MHz bandwidth and when the bandwidth allocation is greater than 5 MHz, at least 400 mobile terminals should be supported [13]. The allowed number of inactive users in a cell should be significantly higher.

The LTE system performance design target addresses topics like user throughput, spectral efficiency, mobility and coverage. The LTE user throughput is specified at the average and the 5th percentile of the user distribution [13]. Spectral efficiency was also specified and its design targets are presented in Table 2.1. The baseline that Table 2.1 refers to is Release 6 High-Speed Packet Access (HSPA) as described in [2].

Table 2.1 *- LTE user throughput and spectrum efficiency requirements compared to HSPA [13]*

Performance measure	**Downlink target relative to baseline**	**Uplink target relative to baseline**
Average user throughput (per MHz)	3x-4x	2x-3x
Cell-edge user throughput (per MHz, 5^{th} percentile)	2x-3x	2x-3x
Spectrum efficiency (bits/s/Hz/cell)	3x-4x	2x-3x

In LTE, the mobility requirements are set for different speeds of the mobile terminal. The best performance is targeted for mobile terminals with a low speeds, i.e. 0 till 15 km/h, while it should provide a reasonable performance with only a slight degradation for higher speed till 120 km/h. For speeds that are higher than 120 km/h, the system should be able to maintain the connection across the cellular network. The

maximum terminal speed that the cellular network can handle is 350 km/h, or it could even reach 500 km/h depending on the operating frequency [13].

The coverage requirements specify the cell ranges in LTE networks. In a non-interference-limited scenario where the previously mentioned design targets like the spectrum efficiency, user throughput and mobility requirements are fulfilled, the cell range can reach up to 5 km [13]. A slight degradation in the user throughput is tolerated for cells up to 30 km in range but more degradation in the spectral efficiency is accepted when maintaining the mobility requirements [13]. For cell ranges that reach 100 km radius, no performance requirements are stated in the specifications [13].

2.4.2. Wireless Local Area Network (WLAN)

Based on IEEE 802.11 family of standards and marketed under the Wi-Fi brand name, WLAN links several devices together wirelessly to form a communication network. The WLAN technology is mainly used for the wireless transmission of Internet Protocol (IP) packets, providing an access to the internet, high performance data rates and a relatively low mobility. Data rates in IEEE 802.11 a/g varies between as low as 6 Mbits/s and reaching rates of 150 Mbits/s depending on parameters like the modulation type and the coding rate. Table 2.2 shows various IEEE 802.11 protocols and some of their respective parameters.

Table 2.2 *– Various IEEE 802.11 protocols and their respective parameters [34]*

Protocol	**Release[19]**	**Operating frequency (GHz)**	**Bandwidth (MHz)**	**Modulation**	**Data rates (Mbits/s)**
802.11 a	September 1999	5	20	OFDM	6, 9, 12. 18. 24, 36, 48, 54
802.11 g	June 2003	2.4	20	OFDM and DSSS	6, 9, 12. 18. 24, 36, 48, 54
802.11 n	October 2009	2.4 and 5	20	OFDM	7.2, 14.4, 21.7, 28.9, 43.3, 57.8, 65, 72.2
			40		15, 30, 45, 60, 90, 120, 135, 150

As it can be seen from Table 2.2, the same IEEE 802.11 protocol can have different data rates depending on the parameters that are selected. For instance, increasing the bandwidth for the case of the 802.11 n protocols increased the data rate. Additionally, the modulation type and the coding rate are the main parameters that are used to change the data rate. Table 2.3 shows an example of the different coding rates and modulation types that affect the data rate of the IEEE 802.11 a/g protocol.

Table 2.3 *– IEEE 802.11 a/g code rate, modulation type and their corresponding data rate [25]*

Data rate (Mbits/s)	Code rate	Modulation Type
6	1/2	BPSK
9	3/4	BPSK
12	1/2	QPSK
18	3/4	QPSK
24	1/2	16-QAM
36	3/4	16-QAM
48	2/3	64-QAM
54	3/4	64-QAM

In WLAN, the OFDM standards use 52 subcarriers for a symbol, where 4 of them serve as pilot subcarriers used to track the residual carrier frequency offset remaining after the initial frequency correction during the packet's training phase [16]. The rest of the subcarriers carry user data, where the data rates are varied according to the parameters listed as an example of IEEE 802.11 a/g protocol in Table 2.3. The GI's length is 1/8th the OFDM symbol duration length which is set to span the time of 4 µs. Such GI length will allow the use of the WLAN technologies in indoor environments as well as outdoor environments; although directional antennas should be deployed to decrease the delay spread and to increase the range, therefore, the subcarrier spacing is 312.5 kHz operating in a 3-dB bandwidth of 16.56 MHz.

Such OFDM symbol configuration is being modified in the latest IEEE 802.11 ac WLAN standard which can provide a theoretical multi-station throughput of at least 1 Gbits/s and a single throughput of at least 500 Mbits/s [16]. The modifications of the

WLAN standards include a higher Radio Frequency (RF) bandwidth that can optionally reach 160 MHz, more MIMO spatial streams and high density modulation (256-QAM) [16]. The standard is expected to have the final 802.11 working group approval and publication on early 2014 [19].

2.4.3. Digital Video Broadcasting – Terrestrial (DVB-T)

First published in the UK in 1998, DVB-T is a broadcast transmission standard that transmits Moving Picture Experts Group (MPEG) transport stream [14]. DVB-T uses OFDM modulation to transmit its data. The data subcarriers are arranged to form an OFDM symbol, and 68 OFDM symbols are arranged to form and OFDM frame. Two modes of transmission exist in the DVB-T standards: 2K and 8K modes. The 8K mode has 6817 OFDM subcarriers in one OFDM symbol, while the 2K mode has 1705. At different carrier spacing, both modes have a 7.61 MHz bandwidth. The GI length in both modes can vary between 1/4 and 1/32 the useful time of one OFDM symbol. In addition of the transmitted data, an OFDM symbol in DVB-T contains scattered pilot cells, continual pilot carriers and Transmission Parameters Signaling (TPS) carriers that are used in an OFDM frame, frequency and time synchronization, channel estimation, transmission mode identification and to estimate the phase noise in an OFDM symbol [14]. Similar to other standards that deploy OFDM as a modulation scheme, the useful bitrate depends on the code rate, the guard interval size and the subcarrier modulation type, varying between 4.98 Mbits/s data rate that has 1/2 code rate, QPSK subcarrier modulation and 1/4 guard interval ratio till 31.67 Mbits/s having a 7/8 code rate, 64-QAM subcarrier modulation and 1/32 guard interval ratio irrespective of the transmission mode [14].

3. PHASE NOISE IN OFDM AND OFDMA

Now that a general overview of OFDM and OFDMA and their limitations were presented in Chapter 2, the main topic that this thesis investigates, namely phase noise in OFDM and OFDMA systems, is presented in this chapter. Some of the modeling and characterization of phase noise in the literature is analyzed along with its effect on OFDM and OFDMA signals.

3.1. Phase noise modeling

Amongst the various non-idealities within an OFDM transceiver, phase noise of the local oscillator is one of the most significant and complex of them. Many studies, such as [31] and [26], have investigated and characterized mathematical models for the phase noise phenomenon and further applied them on the transceiver modeling to evaluate their performance. A real oscillator signal, when phase noise is denoted by the term $\varphi(t)$, can be written as

$$s_R(t) = Acos(w_c t + \varphi(t)), \tag{3.1}$$

and for a complex signal can be written as

$$s_{IQ}(t) = Ae^{(j(w_c t + \varphi(t)))}, \tag{3.2}$$

where *A* is the amplitude and w_c is the angular frequency of the oscillating signal. As it can be seen in (3.1) and (3.2), $\varphi(t)$ is time varying. This property, along with randomness, is what makes the estimation of phase noise a complicated procedure. Ideally, $\varphi(t)$ should be zero and the oscillator angular frequency should be locked to w_c. However; this is not the case in practice. In this thesis, $\varphi(t)$ will be modeled using the Free-Running Oscillator (FRO) model, while more practical and complicated phase noise modeling such as the Phase-Locked-Loop (PLL) model exists, but is left out from this thesis for simplicity. The FRO model is a simple mathematical realization that models the phase noise effect as a random process called Brownian motion or a Wiener process [18]. It can be written as

$$\varphi(t) = \sqrt{c}B(t), \tag{3.3}$$

where *B(t)* is the time varying standard Brownian motion [18] and *c* represents the inverse of the relative oscillator quality which is referred to as the diffusion rate of the Brownian motion process. The FRO model is easy to implement in a discrete-time simulation since (3.3) can be rewritten as

$$\varphi_n = \sqrt{c}B(nT_s) \tag{3.4}$$

where T_s is the sampling time interval. Statistically, the Brownian motion follows a normal distribution which can be characterized with the property

$$B(nT_s) - B\big((n+1)T_s\big) \sim N(0, cT_s). \tag{3.5}$$

$N(\mu, \sigma^2)$ here represents the normal distribution, where μ and σ^2 are the mean and the variance of the normal distribution respectively. Equation (3.5) means that a sampled FRO process can be generated by using a cumulative sum of the realizations of a random distribution with a zero-mean and variance cT_s. The variance of the normal distribution in this case increases linearly as a function of time, meaning that the phase process is non-stationary. Despite the non-stationary nature of the FRO phase process, the phase exponential term labeled as $s_{IQ}(t)$, and thus the oscillator model, is nonetheless stationary [26].

Ideally, the spectral components of an oscillating signal is an impulse function located at the oscillating frequency f_c. However, due to the phase noise effect, the frequency response of the oscillating signal will no longer be an impulse at f_c, and new dispersed frequency components around the oscillating frequency will appear. To demonstrate this effect mathematically, the Power Spectral Density (PSD) of the real time oscillating signal which is written in (3.1) will be deduced by applying the Fourier transform of its autocorrelation function. The autocorrelation function of the real time oscillating signal is

$$\begin{aligned} P_{ss}(t, t+\tau) &= E\{s_r(t)s_r(t+\tau)\} = E\big\{\cos\big(w_c t + \varphi(t)\big)\cos\big(w_c(t+\tau) + \varphi(t+\tau)\big)\big\} \\ &= \frac{1}{2}e^{-\frac{1}{2}c|\tau|} \times \cos(w_c\tau), \end{aligned} \tag{3.6}$$

where $E\{.\}$ and $|.|$ here denote the statistical expectation operator and the absolute value operator respectively. The amplitude value *A* of the oscillating signal is set to unity for simplicity. The result of (3.6) implies that the autocorrelation function of a real

oscillating signal has zero-mean and time dependent, meaning that it is a stationary process as noted earlier. Now taking the Fourier transform of (3.6) will result in

$$V_s(w) = \int_{-\infty}^{\infty} P_{ss}(t, t+\tau)\cos(w\tau)\,d\tau = \frac{1}{2}\frac{c/2}{(c/2)^2+(w+w_c)^2} + \frac{1}{2}\frac{c/2}{(c/2)^2+(w-w_c)^2}. \quad (3.7)$$

To simplify the resulting frequency response of the result in (3.7), some assumptions which agree with a typical practical condition of the oscillator and the phase noise process are taken into account. These assumptions are relatively large oscillation frequency w_c and a relatively small diffusion rate *c*. Equation (3.7) can then be written as

$$V_s(\Delta w) \approx \frac{c/2}{(c/2)^2+(\Delta w)^2}, \quad (3.8)$$

where $\Delta w = w - w_c$ is the frequency deviation from the nominal oscillation frequency. Consequently, to find a more tangible way of describing the phase noise process, the 3-dB bandwidth of the phase noise is derived from (3.8) and can be written as

$$\beta = \frac{c}{4\pi}, \quad (3.9)$$

where β here is in radians. Subsequently, the phase noise process is controlled in this thesis by varying its 3-dB bandwidth value β.

3.2. Effect of Phase Noise on an I/Q signal

Generally, an I/Q signal is a complex signal that carries an in-phase (I component) and a quadrature phase (Q component). A complex I/Q signal can be written as follows

$$s(t) = s_I(t) + js_Q(t), \quad (3.10)$$

where $s_I(t)$ is the I component and $s_Q(t)$ is the Q component. The modulation of the complex signal $s(t)$ is done by multiplying it by two orthogonal modulating signals. The orthogonality of the carriers insures the separation of the modulated complex signal at the receiver. A modulated I/Q signal can be represented as follows

$$m(t) = s_I(t)\cos(w_c t) - s_Q(t)\sin(w_c t). \quad (3.11)$$

Equation (3.11) assumes that the modulating signals are perfectly locked to the desired oscillating frequency, while this is not the case in practice. To give (3.11) a

more practical sense, the phase noise terms are added in the modulation phase and (3.11) becomes

$$m_{\varphi}(t) = s_I(t)\cos(w_c t + \varphi(t)) - s_Q(t)\sin(w_c t + \varphi(t)). \tag{3.12}$$

where $\varphi(t)$ is the phase noise. Sensibly, at the reception of $m_{\varphi}(t)$, the oscillating frequency of the demodulating signals will likewise suffer from the phase noise effect; however, this effect will be omitted in this analogy for simplicity. The operations applied on the modulated signal at the receiver side for the I component case will be

$$\hat{s}_I(t) = \text{LPF}\{m_{\varphi}(t)\cos(w_c t)\} = \frac{1}{2}[s_I(t)\cos(\varphi(t)) + s_Q(t)\sin(\varphi(t))], \tag{3.13}$$

where $LPF\{.\}$ denotes an ideal lowpass filtering operation. Subsequent, the received Q component can be written as

$$\hat{s}_Q(t) = \text{LPF}\{m_{\varphi}(t) - \sin(w_c t)\} = \frac{1}{2}[s_Q(t)\cos(\varphi(t)) - s_I(t)\sin(\varphi(t))]. \tag{3.14}$$

Now that both the I and Q components are defined, rearranging the received signal based on (3.10) to be clearly written as a function of phase noise will be

$$\begin{aligned}\hat{s}(t) &= \hat{s}_I(t) + j\hat{s}_Q \\ &= s_I(t)[\cos(\varphi(t)) - j\sin(\varphi(t))] + js_Q(t)[\cos(\varphi(t)) - j\sin(\varphi(t))] \\ &= s_I(t)e^{-j\varphi(t)} + js_Q(t)e^{-j\varphi(t)} = s(t)e^{-j\varphi(t)}.\end{aligned} \tag{3.15}$$

The result in (3.15) shows that the phase noise effect on a general I/Q modulated signal can be perceived as the multiplication of the transmitted complex signal by a complex conjugate of a complex exponential that carries the phase noise information in its argument. As it was mentioned earlier, the phase noise effect at the receiver was omitted for the simplicity of the analogy, however, in practice; the result of (3.15) is yet multiplied by another complex exponential, making the overall phase noise effect at the receiver even stronger.

3.3. Effect of Phase noise on OFDM signals

As it can be seen from (3.15), the effect of phase noise on an I/Q modulated complex signal can be viewed as a multiplication of the complex signal by an exponential function that carries the time varying phase noise in its argument. This can be further applied on OFDM subcarriers where each one of them is an M-QAM modulated data

symbol. Going back to (2.1) where the *m*th OFDM symbol was defined, the effect of phase can be written as

$$x_{n,\varphi(nT_s)}(m) = x_n(m)e^{-j\varphi(nT_s)}, \tag{3.15}$$

where $x_{n,\varphi(nT_s)}(m)$ is the transmitted *m*th OFDM symbol including the phase noise effect, $x_n(m)$ is the *m*th OFDM symbol and $\varphi(nT_s)$ is the discrete-time phase noise function with T_s representing the sampling time and $n \in [0, N-1]$ of the total N OFDM symbol subcarriers. Figure 3.1 shows an OFDM transceiver diagram that shows the phase noise effect added in the transmission and reception stages.

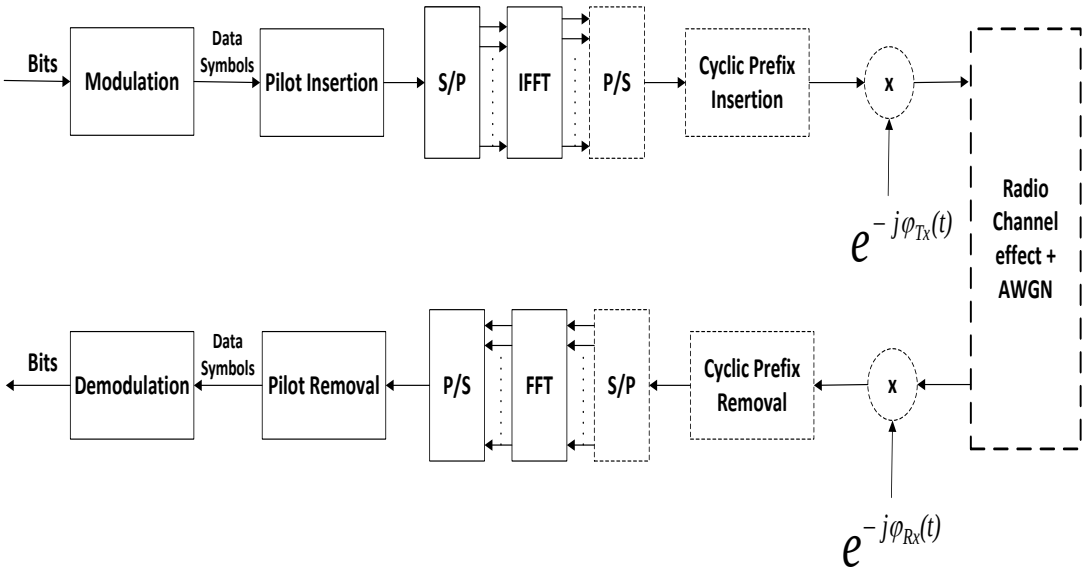

Figure 3.1 *– OFDM baseband transmission and reception chain. The phase noise effect is added in the transmission and reception stages resulting into a practical scenario.*

To illustrate the effect of phase noise in an OFDM symbol, Figure 3.2 shows an example of a constellation plot of an OFDM symbol that experienced the phase noise effect at the transmission stage. In this example, 16-QAM modulation was used where the number of data subcarriers used is $N = 582$ and the phase noise 3-dB bandwidth β is 50 Hz. As it can be seen from the figure, the constellation is slightly rotated due to the average value of the added phase noise for this particular symbol. This effect is referred to as the Common Phase Error (CPE). Additionally, the constellation points are scattered due to the ICI effect that the phase noise causes in multi-carrier signals.

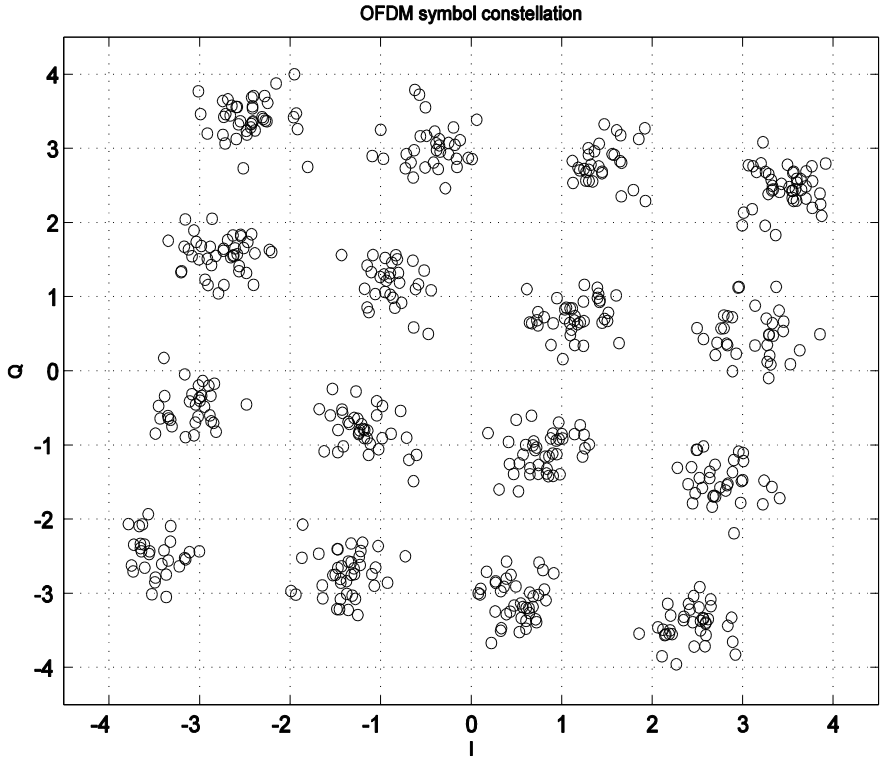

Figure 3.2 *– An OFDM symbol's constellation plot with phase noise. The subcarriers are 16-QAM modulated data symbols. The phase noise 3-dB bandwidth is* $\beta = 50Hz$.

Additionally, the effect of phase noise with its CPE and ICI components for a received signal after it has gone through the DFT procedure in the receiver can be written as

$$R_k(m) = X_k(m)H_k(m)J_0(m) + \sum_{l=0,l\neq k}^{N-1} X_l(m)H_l(m)J_{k-l}(m) + Z_k(m) \qquad (3.16)$$

where $R_k(m)$ and $X_k(m)$ are the received and transmitted kth OFDM symbols respectively, $H_k(m)$ is the channel's frequency domain response, $J_k(m)$ is the frequency domain phase noise complex exponential and $Z_k(m)$ is the frequency domain additive white Gaussian noise. The first term of (3.16) is responsible for the rotation of the constellation in Figure 3.2 and can be compensated for by estimating $J_0(m)$, while the second term is responsible for the ICI effect. The next chapter discusses the methods used to estimate and compensate the phase noise effect in an OFDM symbol.

3.4. Effect of Phase Noise on OFDMA signals

Now that the effect of phase noise on OFDM signals is explained, the analysis is further expanded to include the OFDMA case since it is the main aim of this thesis. Generally, a signal experiences two types of phase noise effects, an in-band and an out-of-band one. If there are no communication signals that are active near an OFDM signal operating at a certain frequency, interference due to phase noise is bounded to the in-band effect and is dealt with accordingly; however, this is not the case in OFDMA. As explained earlier, an OFDMA signal contains the data of several users that independently experience different effects. For instance, each user will have a different effect concerning phase noise characteristics, channel effects and different powers at the reception. This exposes the OFDMA signal users to phase noise induced out-of-band interference.

An example of a contiguous subcarrier assignment scenario in an OFDMA symbol illustrating the out-of-band interference is depicted in Figure 3.3. The power spectrum of an OFDMA symbol is shown with and without the inclusion of the effect of phase noise. An OFDMA user is caught in the middle between two edge users having significantly higher powers where the power difference is Ψ = 24 dB. Additionally, the edge users suffer from the phase noise effect where the 3-dB phase noise bandwidth is 500 Hz. 16-QAM modulation was used to modulate the data symbols and the powers of 500 OFDMA symbols where averaged to smooth out the power spectrum in order to clarify the spreading effect. An AWGN channel was used in the simulation to restrict the attribution of the spreading effect to the boosted phase noise induced spreading effect. The phase noise effect along with the power difference between the edge users and the middle one have caused a substantial undesirable spread from the edge users on the subcarriers of the middle user as seen in Figure 3.3.

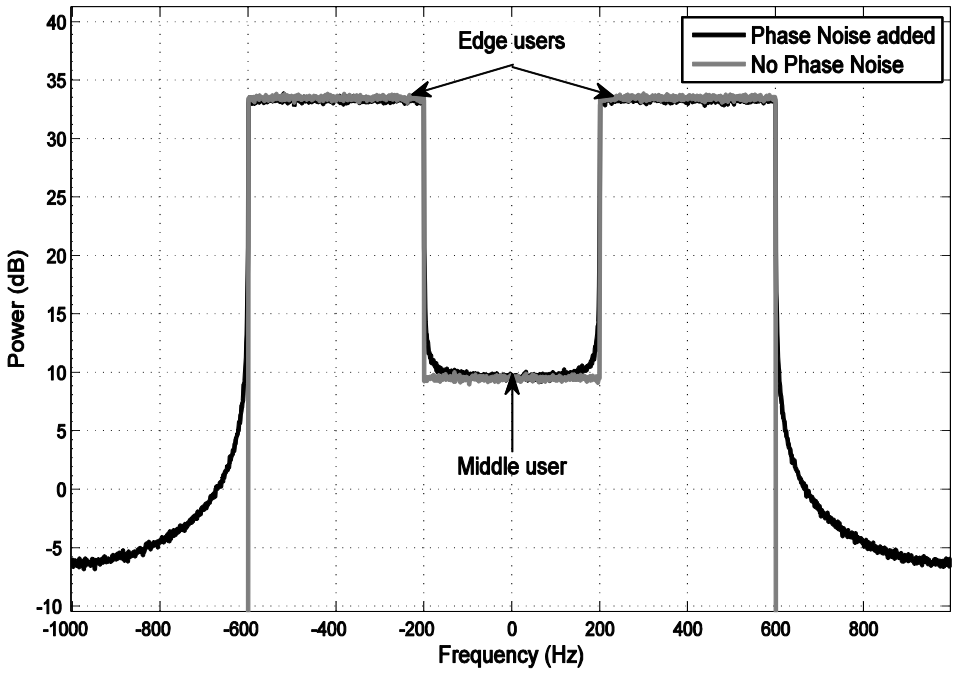

Figure 3.3 *- OFDMA symbol showing frequency spread on the middle. Ψ = 24 dB and $\beta = 500Hz$ for the edge users.*

The choice of such high values of β and Ψ is to clearly show the spreading effect in Figure 3.3. The out-of-band interference relating to a certain user in an OFDMA signal is theoretically formulized in the next chapter.

4. PHASE NOISE ESTIMATION AND MITIGATION IN OFDM AND UPLINK OFDMA

As previously discussed, OFDM receivers are highly sensitive to frequency errors due to the orthogonality condition between subcarriers that should be maintained. For this reason, phase noise estimation and mitigation algorithms in OFDM receivers have been studied in the literature [27], [29], [30], [31], [32]. At the beginning, only the Common Phase Error (CPE) estimation and mitigation method was considered and studied in [24]. The mitigation of CPE will leave the effect of ICI present in the received OFDM waveform which implies that a compensation technique should be applied to mitigate its effect. An example of an ICI estimation and mitigation method was demonstrated in [22]. It is a frequency domain approach to estimate the low-pass (centermost) frequency components of the ICI, while in the same publication, iterations were applied to improve the ICI estimation.

Another study of relevance to this thesis is the one done in [23], where the effect of phase noise in OFDM-based Amplify-and-Forward (AF) relay networks was analyzed and a reduced-complexity joint channel and phase noise estimation was performed. This study is of importance since it deals with an uplink OFDM scenario similar to the phase noise affected OFDMA scheme studied in this thesis.

The CPE and ICI estimation techniques will be explained in this chapter since they will be applied as methods of phase noise estimation in uplink OFDMA. This chapter will present several phase noise estimation and mitigation techniques for an OFDM signal and then proceeds to explain a methodology to use these estimation techniques in the case of estimating and mitigating the phase noise in an OFDMA signal.

4.1. CPE Estimation

The CPE is an effect that OFDM waveforms suffer from due to the multiplication of these OFDM waveforms with the average value of the phase noise. Estimating the value of this CPE is merely estimating the common complex multiplier of the phase noise that affects an OFDM symbol. The pilot data that is inserted in the OFDM symbol is used

for a Least Squares (LS) estimation of the CPE, and this CPE estimation during the *m*th OFDM symbol can be written as [35]

$$\hat{J}_{0,m} = \frac{\sum_{k\epsilon S_p} R_k(m) X_k^*(m) H_k^*(m)}{\sum_{k\epsilon S_p} |X_k(m) H_k(m)|^2}. \quad (4.1)$$

where $R_k(m)$ is the received pilot data, $X_k(m)$ is the known pilot data (when $k \in S_p$), $H_k(m)$ is the channel transfer function, $\hat{J}_{0,m}$ is the DC bin of the frequency domain phase noise complex exponential (estimated) and S_p represents a set of pilot data. The operators "*" and "|.|" denote the complex conjugate and the absolute value of a complex number respectively. The LS estimation is used for its computational simplicity. The CPE effect is then simply mitigated by a simple division of the received OFDM symbol with the CPE estimate.

4.2. ICI Estimation

The ICI is the most complex part of the phase noise effect on an OFDM symbol; therefore its estimation is generally more complex than the estimation of CPE. ICI is manifested by the variation around the mean of the phase noise. Therefore, it is said that ICI is the effect caused by the non-DC part of the phase noise. Namely, after the CPE compensation, the remaining part of the phase noise is similar to the original phase noise effect except for the fact that its mean is approximately zero. Consequently, it can be said that the zero-mean phase noise causes ICI. There are several ways to estimate the ICI effect on an OFDM symbol, and some examples are the studies performed in [3], [4], [5], [6], [7], [8], [9], [10], [22], [29], [30], and [31], where few of them are shortly presented in this thesis. The first and the simplest one is proposed in [31], while more accurate attempts to estimate the ICI effect are proposed in [22]. In this thesis, the method presented in [22] will be used as a part of the method proposed for phase noise mitigation in OFDMA systems, while other more accurate ICI estimation method in OFDM systems, presented in [31], is only reviewed in this thesis as part of the literature.

4.2.1. LI-CPE Estimation

First proposed in [31], the Linear Interpolation – Common Phase Error (LI-CPE) is a method to estimate the ICI effect using previously estimated CPE values. The method

simply interpolates the consecutive CPE estimates from the middle of an OFDM symbol to the next one. In other words, the interpolation in LI-CPE estimation interpolates the average values of phase noise using a linear interpolation. The linear interpolation was selected for this method due to its relative simplicity and more importantly, its selection was motivated by the fact that the linear interpolation is approximately the optimal way to do an interpolation between two points in a Wiener process [26]. Figure 4.1 shows the LI-CPE interpolation compared with a CPE estimation of phase noise in 8 consecutive OFDM symbols.

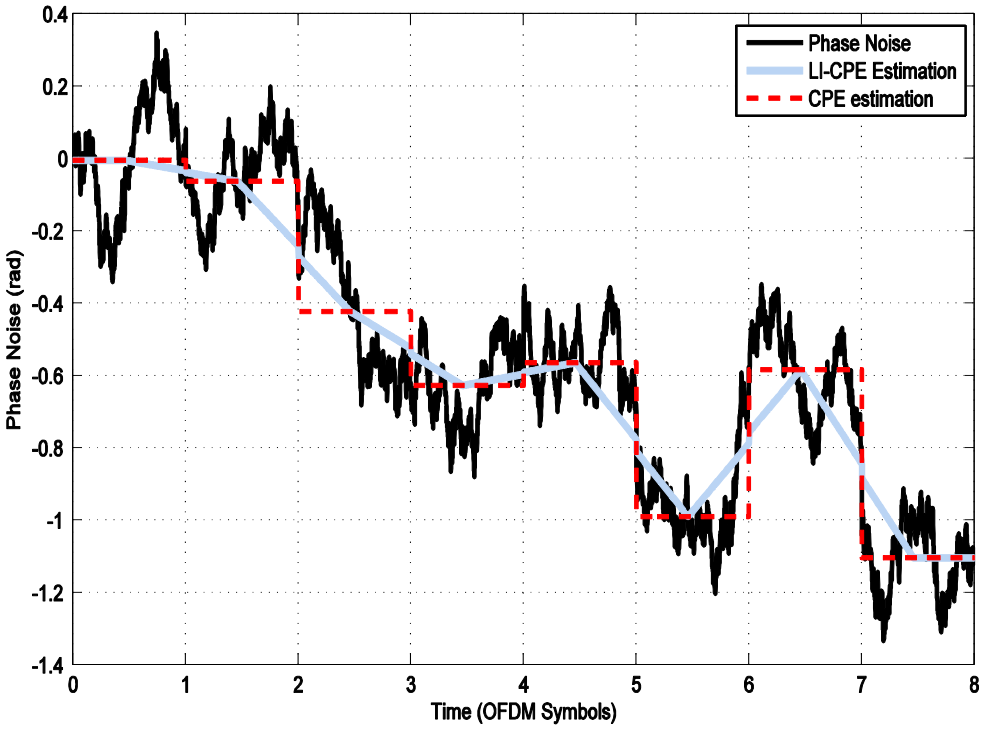

Figure 4.1 *- CPE and LI-CPE estimations of phase noise*

4.2.2. Iterative ICI Estimation

The iterative ICI estimation method is proposed in [22] and has a more accurate estimation of ICI than the LI-CPE method discussed previously. The method requires CPE mitigated OFDM symbols which are used initially and later replaced by ICI mitigated OFDM symbols throughout the rest of the iterations. Additionally, this method approximates the phase noise spectral components assuming that most of the phase noise effect lies within the center-most frequency taps of the phase noise's

spectral components. Analytically, the frequency domain received signal model where the transmitted signal undergoes the effects of the channel and phase noise is

$$R_k(m) = \sum_{l=-u}^{u} X_{k-l}(m)H_{k-l}(m)J_l(m) + V_k(m) = \sum_{l=-u}^{u} A_{k-l}(m)J_l(m) + Z_k(m), \quad (4.2)$$

where $X_k(m)H_k(m)$ are here replaced by $A_k(m)$ for simplicity, and $Z_k(m)$ represents the additive noise combined with the remaining ICI effect that is not accounted for in this method which is outside the spectral components range [-u, u]. P subcarriers are selected with the condition $P \geq 2(u+1)$, and solving for $J_l(m)$ in a matrix form will be in performed in the following way

$$\begin{bmatrix} R_{l_1}(m) \\ R_{l_2}(m) \\ . \\ . \\ . \\ R_{l_P}(m) \end{bmatrix} = \begin{bmatrix} A_{l_1+u}(m) & \cdots & A_{l_1-u}(m) \\ \vdots & \ddots & \vdots \\ A_{l_P+u}(m) & \cdots & A_{l_P-u}(m) \end{bmatrix} \begin{bmatrix} J_{-u}(m) \\ J_{-u+1}(m) \\ . \\ . \\ . \\ J_u(m) \end{bmatrix} + \begin{bmatrix} Z_{l_1}(m) \\ Z_{l_2}(m) \\ . \\ . \\ . \\ Z_{l_P}(m) \end{bmatrix}. \quad (4.3)$$

The previous matrix operations can be written compactly as $\mathbf{R}_{m,P} = \mathbf{A}_{m,u}\mathbf{J}_{m,u} + \mathbf{V}_{m,P}$, where $\mathbf{R}_{m,P}$ and $\mathbf{V}_{m,P}$ are $P \times 1$ vectors and, $\mathrm{J}_{m,u}$ is a $(2u+1) \times 1$ vector and $\mathbf{A}_{m,u}$ is a $P \times (2u+1)$ matrix. Consequently, LS estimate of $\mathbf{J}_{m,P}$ can be found as

$$\hat{\mathrm{J}}_{m,P} = (\mathbf{A}_{m,u}^H \mathbf{A}_{m,u})^{-1} \mathbf{A}_{m,u}^H \mathbf{R}_{m,P.} \quad (4.4)$$

The above equation gives an estimation of the center-most spectral components of phase noise that carry most of the phase noise power. Figure 4.2 shows a realistic example of the ICI magnitude spectrum. The x-axis indicates the indices of the frequency components and shows the range *[-u, u]* where in this case *u*=3.

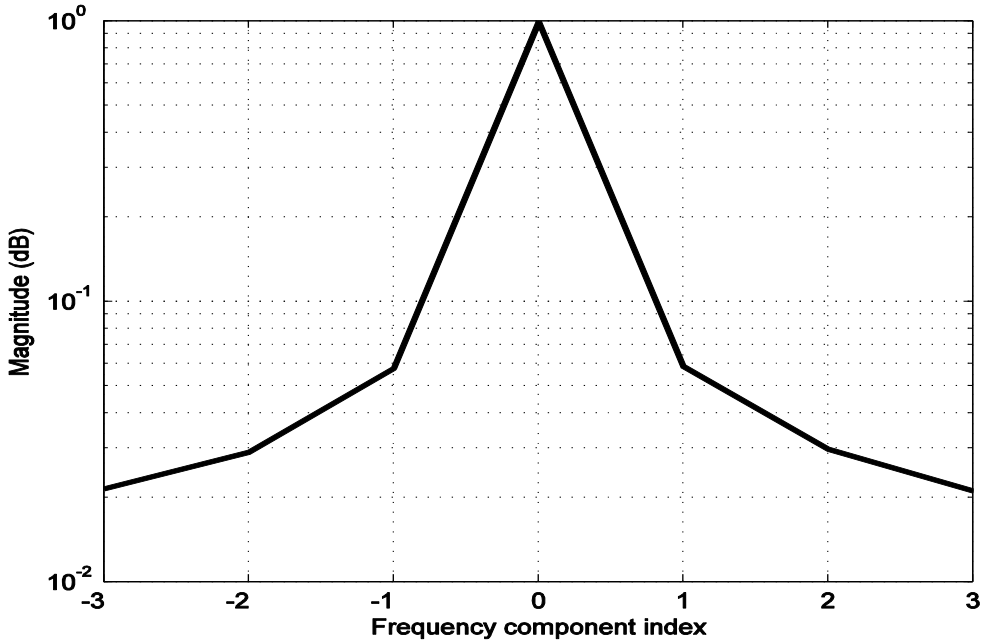

Figure 4.2 *- Averaged estimated ICI magnitude spectrum for u=3*

After the estimation of the center-most frequency components of the ICI, they are transformed to the time domain using an IFFT operation, and the time domain received signals are simply divided in an element by element fashion to compensate the phase noise effect. Another way of compensation can be performed by applying the de-convolution operation between the received discrete Fourier transformed OFDM symbol and the estimated center-most frequency components of the ICI. Finally, these phase noise compensated and detected OFDM signals are used in an iterative fashion to improve the ICI estimation. In this thesis, up to three iterations are implemented, after which the improvement becomes relatively minimal [26].

4.2.3. LI-TE Estimation

Linear Interpolation – Tail Estimation (LI-TE) is a method used to improve the previously discussed iterative ICI estimation. The author in [26] noticed the poor performance of the iterative ICI estimation at the edges of the OFDM symbol, and applied linear interpolation over the edges of the OFDM symbols. This poor performance at the edges is attributed to the FFT truncation performed in the estimation of the ICI spectral components. Linear interpolation was selected for the same reasons mentioned in the LI-CPE method. The interpolation starts from the last reliable phase noise estimation data point to the first reliable one in the next OFDM symbol. In [26], it was empirically determined that around 15% of the OFDM symbol length is substituted

with the interpolation values at the edges. Figure 4.3 shows an example of the ICI and LI-TE phase noise estimation results for several OFDM symbols.

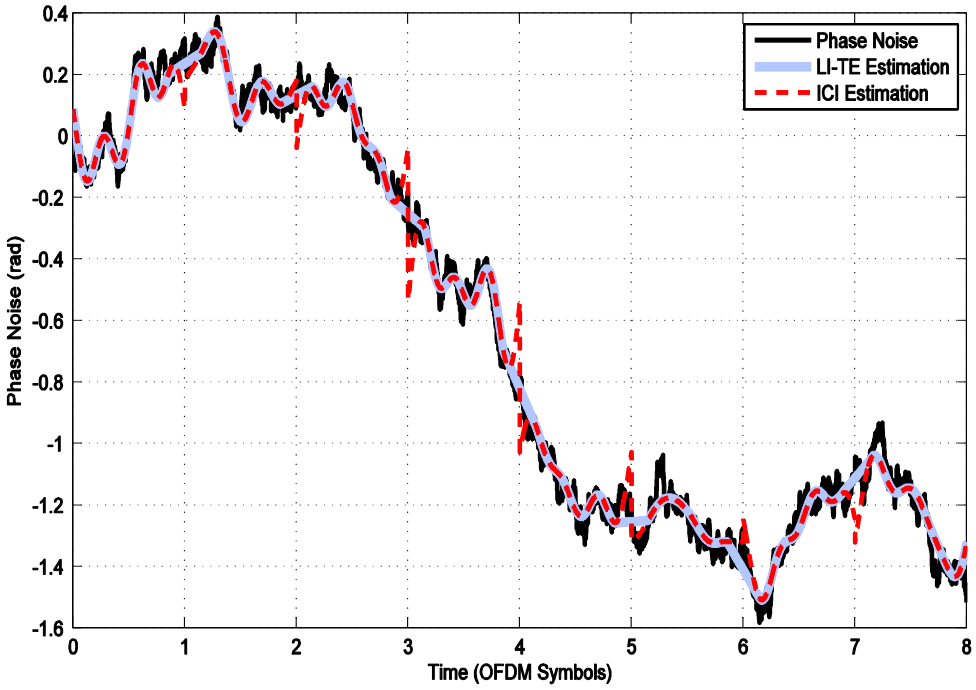

Figure 4.3 *- ICI and LI-TE phase noise estimation techniques*

4.3. Contribution to Phase Noise Estimation in OFDMA

After going through several existing techniques of phase noise estimation and mitigation methods for OFDM waveforms, the use of these techniques is now applied on an OFDMA uplink case with transmitter phase noise.

As pointed out at the beginning of this chapter, a study was performed in [23] to analyze the effect of phase noise in an OFDM-based Amplify-and-Forward (AF) relay networks. The study shows that the use of an AF relay is not beneficial when compared to a direct transmission scheme if the phase noise level surpasses an allowable upper bound limit, and the AF scheme's performance can be improved by using a reduced-complexity joint channel and phase noise estimation technique. The scenario studied in [23] is not similar to the OFDMA case studied in this thesis but is of relevance since it deals with the phase noise effect in uplink OFDM, although the derived phase noise estimation and mitigation method in this thesis is derived independently.

The issue of phase noise in OFDMA is not solely confined to the effects of CPE, ICI and the degradation they cause to the overall system performance, but now a new

problem rises and should be addressed. In a contiguous user subcarrier assignment, the combination of the varying powers for each user and phase noise affects the neighboring users in an OFDMA symbol [28]. This effect is manifested by a spectral spread of subcarriers of one OFDMA user on the top of the subcarriers of another user, creating what can be conveniently called Inter-User Interference (IUI). Figure 3.3 in the previous chapter illustrates a specific scenario of an OFDMA symbol structure and depicts the phase noise induced spreading effect for an uplink case.

The following equations formulate the phase noise induced spreading effect of the edge users on the middle one for an Uplink case. The receiver phase noise is assumed to be non-existent at this stage for simplicity and is only confined to the transmitting Mobile Stations (MS). In this analogy, two equations where deduced since there are two adjacent users contributing to the spread, one on the left and the other is on the right of the middle user. The equations are

$$R_{l\gamma,M+x}(m) = R_{l,M+x}(m) + H_{l,M+x}(m)\sum_{k=x}^{M-1} X_{l,k}(m)J_{l,k-M-x}(m), \quad (4.5)$$

$$R_{r\gamma,2M-x-1}(m) = R_{r,2M-x-1}(m) + H_{r,2M-x-1}(m)\sum_{k=2M}^{3M-x-1} X_{r,k}(m)J_{r,k-2M+x+1}(m), \quad (4.6)$$

where $R_{l\gamma}(m)$ and $R_{r\gamma}(m)$ are the received middle user *mth* symbol with IUI from the left and right users respectively, $R_l(m)$ and $R_r(m)$ are the received middle user *mth* symbol without IUI from the left and right users, respectively. X_l and X_r are the frequency domain transmitted left and right OFDMA symbols respectively. J_l and J_r are the frequency domain phase noise for the left and right users respectively and H_l and H_r are the frequency responses of the channels for the left and right users respectively. $R_l(m)$ and $R_r(m)$ already contain the channel and phase noise effects which can be classified as in-band effects. The rest of the components in (4.5) and (4.6) represent the out-of-band spread of the adjacent users which can be referred to as IUI.

In (4.5), (4.6) and the following (4.7) and (4.8), the IUI components are indexed by *k* and the number of IUI components is limited by x where $x \in [0, u-1]$ which indexes the effect of the phase noise spread on the adjacent middle user. The parameter *u* is the phase noise side components length in the frequency domain as illustrated in Figure 4.2. For simplicity, it is assumed that each user has an equal number of subcarriers denoted by *M* and the subcarrier assignment method is contiguous and similar to the case depicted in Figure 3.3. For (4.5) and (4.6), the scenario is not practical as the full

knowledge of the phase noise frequency components is assumed where and the IUI affects the entire middle user's bandwidth and is not restricted by the parameter *u*. The IUI is the result of the convolutions between the transmitted symbols and the frequency domain phase noise components of the adjacent users, which are finally multiplied by the channel frequency responses of the respective users.

In this thesis, a method that addresses the estimation of the main phase noise induced spreading components at the edges of the middle user is developed. The method uses the CPE and ICI estimation methods that were discussed previously. The method starts with estimating the spread caused by the edge users' subcarriers on top of the middle user's subcarriers. After the phase noise spread is estimated, it is removed by subtracting the spread estimations from the edge subcarriers of the middle user. Finally, after the phase noise spread is removed from the middle user subcarriers, its own phase noise is estimated and compensated. Equations (4.7) and (4.8) represent the spread caused by the phase noise of the edge users' subcarriers

$$\hat{S}_{l,x}(m) = \widehat{H}_{l,M+x}(m) \sum_{k=M-u+x}^{M} \hat{X}_{l,k}(m)\, \hat{J}_{l,k-M-x}(m), \tag{4.7}$$

$$\hat{S}_{r,x}(m) = \widehat{H}_{r,2M-x-1}(m) \sum_{k=2M+1}^{2M+u-x} \hat{X}_{r,k-1}(m) \hat{J}_{r,k-2M+x}(m), \tag{4.8}$$

where $\hat{S}_{r,x}(m)$ is the estimated spread at the edges of the middle user on the right side, $\hat{S}_{l,x}(m)$ is the spread at the edges of the middle user on the left, $\hat{X}_r(m)$ are the detected frequency domain data symbols after ICI compensation of the right user, $\hat{X}_l(m)$ are the detected symbols after ICI compensation of the left user, $\hat{J}_r(m)$ are the estimated center-most frequency components of the right user and $\hat{J}_l(m)$ are the estimated center-most frequency components of the left user. Finally, $\widehat{H}_r(m)$ and $\widehat{H}_l(m)$ are the channel estimations of the right and left users respectively where their indices overlap with the middle user indices. From (4.7) and (4.8), it is evident that *u*, which denotes the estimated phase noise side components length in the frequency domain as illustrated in Figure 4.2, is the decisive factor for the length of the IUI estimation on the middle user. In this thesis, *u* was selected to be 3 for the reasons explained in section 4.4.

Figure 4.4 shows the block diagram that explains how the phase noise of the middle user is estimated and mitigated. In order to correctly estimate the phase noise of the middle user, the first step is to remove the spread caused by the phase noise of the adjacent users denoted in Figure 4.4 by $\hat{S}_{l,x}(m)$ and $\hat{S}_{r,x}(m)$. The removal of the

spread is done by subtracting $\hat{S}_{l,x}(m)$ and $\hat{S}_{r,x}(m)$ from the received middle user data symbols. After the removal of the phase noise spread caused by the adjacent users, the CPE is estimated and compensated for the middle user. The detected symbols after the CPE compensation are used in the ICI estimation as explained in section 4.2.2. Finally, the channel effect and ICI are compensated for the middle user.

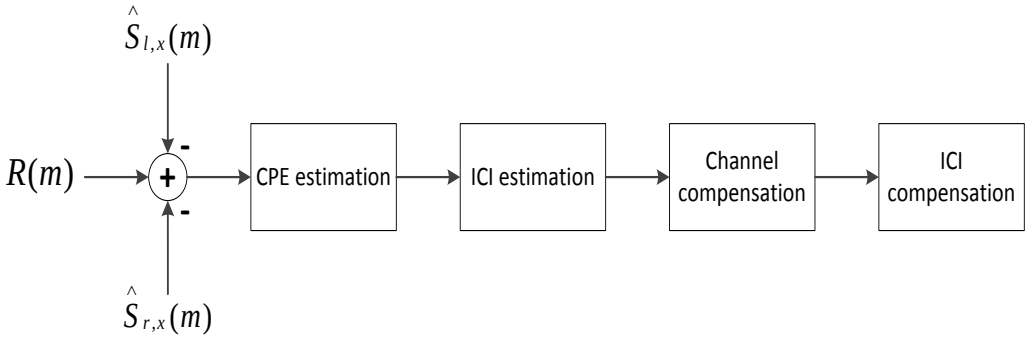

$R(m)$ *is the recived middle user OFDMA mth symbol*

$\hat{S}_{l,x}(m)$ *are the estimated IUI components of the left user*

$\hat{S}_{r,x}(m)$ *are the estimated IUI components of the right user*

Figure 4.4 *- Block diagram describing the symbol detection methodology of the middle user*

4.4. Challenges Faced in Phase Noise Spread Estimation in an OFDMA System

The OFDMA system that is considered in this thesis is based on the contiguous subcarriers mapping. The main objective and contribution in this thesis is to estimate the spread of a user's subcarriers on top of its neighbor's subcarriers due to phase noise and to mitigate this spread. The main limitation for a compensation of IUI is that we can mitigate it only partially. The reason for that is the limited number of phase noise spectral components that we can reliably estimate in practice [22]. Increasing the number of the spectral components to be estimated, e.g., in this method results in erroneous phase noise estimation for these new components since their amplitude is relatively small, and the estimation errors get significant. As previously mentioned in section 4.3, the estimated phase noise side components length in the frequency domain was 3, meaning that only 3 spreading components on both sides of the middle user can be estimated.

Another issue regarding the phase noise spread estimation is the channel estimation beyond the edges of each user's data band. This is an issue because the phase noise spread in the transmitter still experiences the channel effect even beyond the data band. To clarify this problem, an example of the OFDM symbol structure for each user is depicted in Figure 4.5. As it can be seen from the symbol structure, the pilot data that are used in the channel estimations are band limited and do not cover the whole OFDM symbol frequency band. The difficulty here arises when the channel estimation needs to be done beyond the user's band that includes the data to estimate the combined effect of the channel and the phase noise spread on the middle user. To simplify the scenario in Figure 4.5, it is assumed that the middle user does not have a significant spreading effect on the top of the subcarriers of the edge users due to its' relatively low power. The phase noise spreading effect marked in different shades of red show that the spread is severe at the edges of the middle user and its effect decreases as we move away from the edges. The channel frequency response at the phase noise spread locations which correspond to the edge user's channel frequency response should be estimated. The approach to deal with this issue is done by extending the channel frequency response estimates that are attained using the pilot data. These pilot data are the nearest to the middle user and lie at the edges of the edge users. The extensions of these estimates cover the subcarriers of the middle users where the phase noise spread effect is to be estimated. In (4.7) and (4.8), the channel effect was estimated by applying the aforementioned method. A potential drawback of this estimation method is that the further the channel estimation extension goes, the less reliable it becomes. This drawback sets a limit if the phase noise spread estimation is extended to cover more OFDM subcarriers.

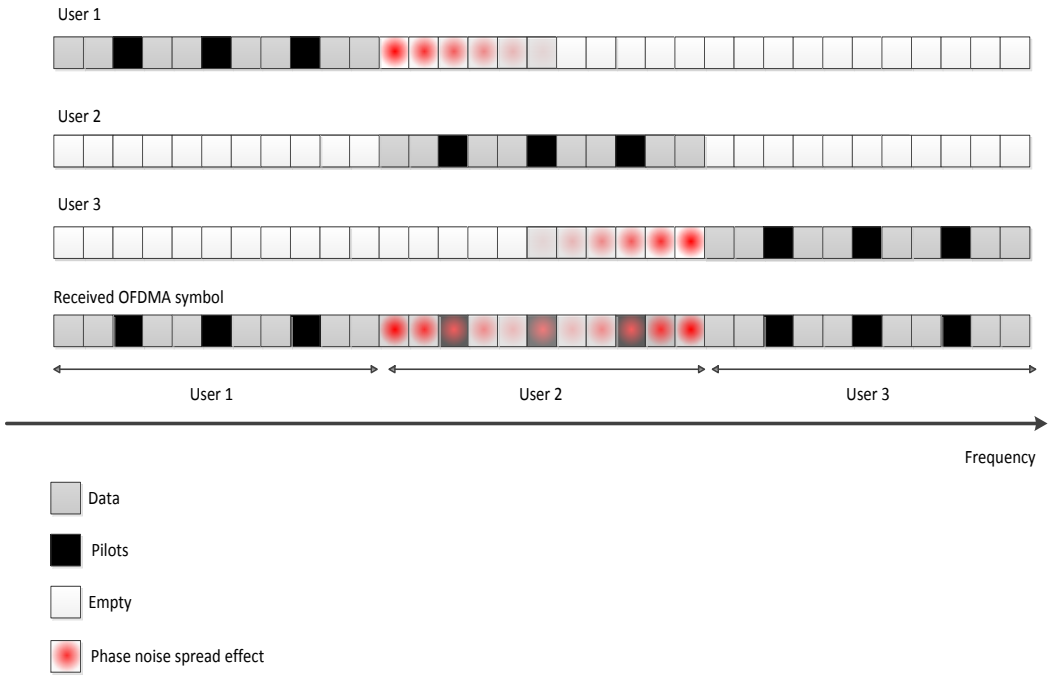

Figure 4.5 *- OFDM symbol structure for each user prior transmission and the received OFDMA symbol after going through the phase noise effect.*

5. SIMUALTIONS AND RESULTS

After introducing the problem and the proposed solution in the previous chapter, the performance simulations are carried out in this chapter. The OFDMA simulation parameters that are applied in the simulations are presented in the first section of this chapter. Next, the verification of an adequate phase noise 3-dB bandwidth in Uplink OFDMA is presented. Subsequently, the simulation results are shown where the OFDMA signal passes through an AWGN channel and a practical ITU-R Vehicular A multipath channel. The results also cover the proposed solution's performance when the phase noise 3-dB bandwidth and the relative power of the edge users are varied.

5.1 Simulation Parameters

In this section, the parameters of the simulation that was used in this thesis are presented. The parameters are listed in Table 5.1.

Table 5.1 *– Simulation parameters of the OFDMA system*

Simulation Parameters	
Number of users	3
Modulation type	16-QAM with Gray
Sampling time	$0.\dot{0}651$ μs
Sampling frequency	15.36 MHz
Number of subcarriers for each edge	582
Number of subcarriers for the middle	36
Total number of subcarriers	1200
FFT/IFFT lengths	2048
OFDMA symbol length	0.78125 ms
Cyclic prefix length	2.6042 μs
Pilot spacing	Every 4^{th} subcarrier

The number of users in this simulation was selected to be 3. This was done to apply the scenario in Figure 3.3 and to simplify the simulator. The sampling time and frequency were taken from the LTE system specifications. The number of subcarriers

selected for the middle user was low. This was done to make the change of the BER performance of the middle user noticeable when the IUI removal method is applied since IUI has the highest overall effect on the users with relatively narrow subcarriers bandwidth allocation. The cyclic prefix length is selected to be higher than the channel's maximum delay spread to cancel the ISI effect. The channel that was used in the simulation is the extended ITU-R Vehicular A channel. Its maximum delay spread spans 39 taps as described in Table 5.2.

Table 5.2 *- Extended ITU-R Vehicular A multipath channel*

Tap	Average relative	Relative delay
1	0	0.0651
2	-1.85	0.1302
5	-3.45	0.3255
6	-0.61	0.3906
12	-7.46	0.7813
17	-6.99	1.1068
27	-11.99	1.7578
39	-16.99	2.5391

The time and frequency domain responses of the ITU-R Vehicular A channel are depicted in Figure 5.1. Notice that these responses are from one realization of the channel but represent typical responses. It can be seen from the previous table and the impulse response of the channel realization that the maximum delay spread is large and stretches to reach 39 taps, the equivalent of almost 2.6 μs. Additionally, it can be noted from the frequency response that the frequency response is selective, which satisfies the desire to pass the simulated signal model through a challenging frequency selective channel.

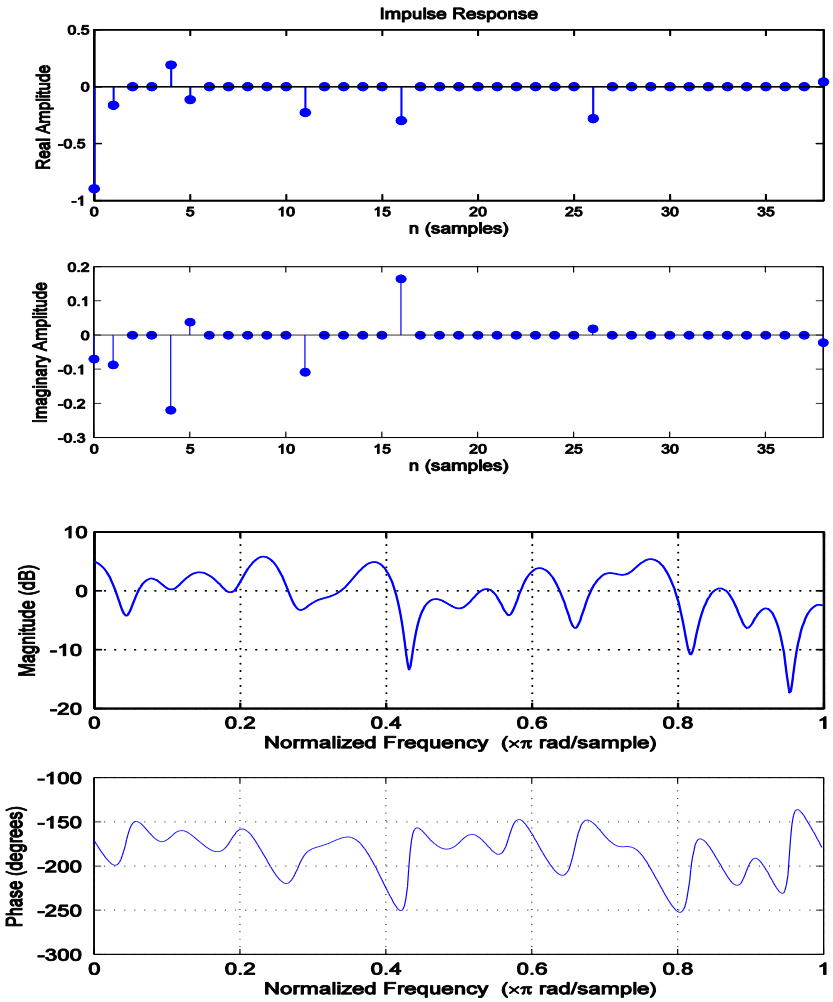

Figure 5.1 *– Impulse (up) and frequency (down) responses of the extended ITU-R Vehicular A multipath channel example realization*

5.2 Verification of a Realistic Phase Noise Level

Before presenting the results, the specifications regarding the transmission of the OFDMA waveforms were checked. This is done to insure that the transmission scenario abides by the specifications of the LTE system so that the results can be considered realistic. The LTE system specifications are retrieved from [1] and are used as a realistic example. The first requirement to check is the Error Vector Magnitude (EVM). The EVM is a quantity that measures the difference between the measured signal and the reference one. In the case of an LTE system, it is measured just after the IFFT block after the measured waveform is corrected by the sample timing offset and RF frequency offset [1]. To measure the EVM, the following equation was applied

$$EVM = \sqrt{\frac{\overline{(|T_s(m) - R_s(m)|)^2}}{\overline{(|R_s(m)|)^2}}}, \quad (5.1)$$

where $T_s(m)$ is the signal after the IFFT block, $R_s(m)$ is the reference modulated signal and the notations $\bar{.}$ and $|.|$ signify the mean and absolute value of a number respectively. According to [1], the EVM limit is 12.5% in a case of 16-QAM modulation. This restriction necessitates a limitation on the amount of phase noise that can be applied on the OFDM transmitted symbol. The limitation is expressed in the 3-dB bandwidth of the applied phase noise which was found to be around 50 Hz. At this phase noise level and in this simulation scenario, the transmission spectrum emission mask requirements are also met [1].

5.3 Results and discussion

After applying the procedure depicted in Figure 4.4, the OFDM system performance of the middle user that is affected by the phase noise induced spread of the adjacent users is tested and compared to the case where nothing is done to remove the IUI. The improvement after applying the developed method is manifested by demonstrating the bit error performance of the middle user. The bit error rate performance is plotted as a function of the SNR for the case of the CPE and ICI mitigation methods with and without the phase noise spread removal.

Figures 5.2 and 5.3 depict the system performances where the transmitted signal undergoes an AWGN and the extended ITU-R Vehicular A multipath channels respectively. The BER vs. SNR of our interest in this study is the one related to the middle user as it suffers from the phase noise induced spreads caused by the neighboring edge users. It is worth mentioning that the SNR of the whole OFDMA waveform is applied with respect to the middle user since in this scenario, the middle user has the lowest power. The simulation was repeated for many times and the average of the BER was calculated for each SNR and then plotted. This was done to ensure that the method works as expected whatever the channel condition is at the edges of the users.

In all of the figures, the plotted BER performances represent the following scenarios: At first, the phase noise of the middle user is estimated using the CPE estimation method and compensated without taking into account the IUI effect caused

by the phase noise of the adjacent users where the curve of this scenario will be named in the following figures as “CPE compensation”. Next, the CPE phase noise estimation and compensation is also applied but this time the IUI caused by the phase noise of the adjacent users is taken into consideration, and the curve for this case is named as “CPE comp. + IUI removal”. Afterwards, the iterative ICI estimation described in section 4.2.2 is applied for the middle user with (“ICI compensated + IUI removal”) and without (“ICI compensated”) considering the IUI effect. Finally, two reference curves are added to the performance comparison. The first, named as “Full IUI removal”, which assumes the full knowledge of phase noise for all users. This means that phase noise induced spread caused by the adjacent users is known as well as the phase noise of the middle user. The second one, named as “Partial IUI removal”, assumes the full knowledge of phase noise of the middle user while having only a partial knowledge of phase noise of the edge users. Partial knowledge of phase noise here means that only a limited number (7 in this case, meaning u=3 on both sides of the DC component) of frequency components of the phase noise are known for the edge users. In addition, for all case studies presented in the following figures, the power difference between the middle and edge users power is set to be 10 dB.

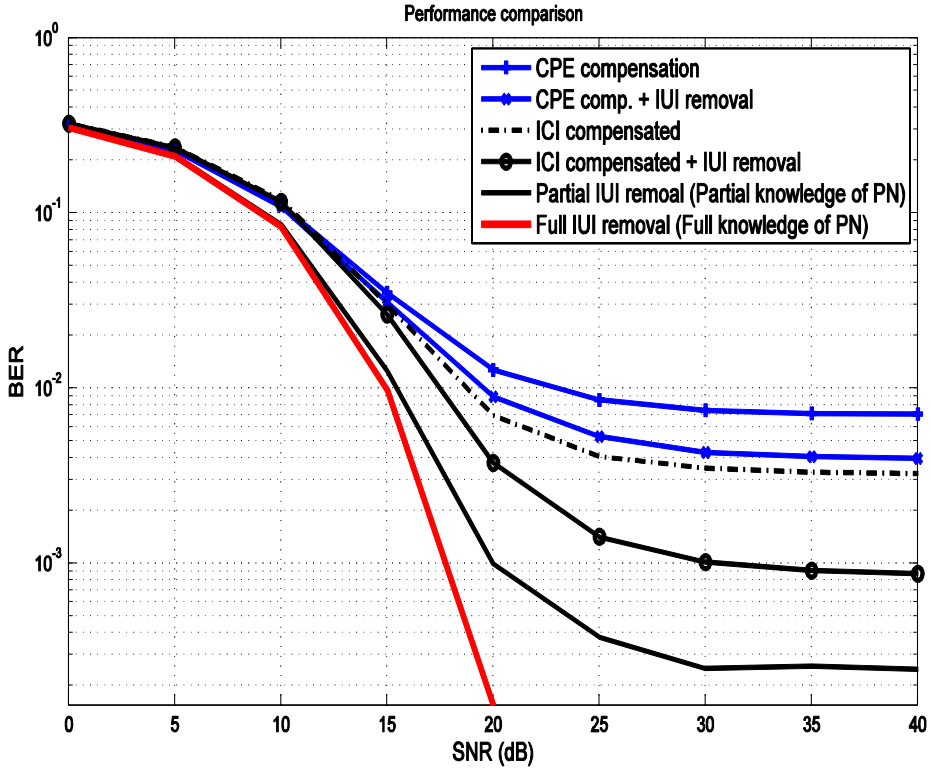

Figure 5.2 *- BER vs. SNR plot for different phase noise mitigation methodologies (AWGN channel, 50 Hz phase noise 3-dB bandwidth), SNR=20 dB.*

In Figure 5.3, the performance of the whole system is degraded when compared to the results presented in Figure 5.2. The reason here is that Figure 5.3 depicts the results of the simulator when the transmitted OFDMA signals pass through the Extended ITU-R Vehicular A multipath channel model. This overall deterioration of the system performance can be attributed to the fact that the middle user, which in its part suffers from IUI from both sides, was selected to have a relatively narrowband bandwidth represented by assigning only 36 subcarriers out of 1200 where the rest of the subcarriers are assigned to both edge users. At this stage, the channel effect is assumed to be known at the receiver, and channel estimation was not performed. Interestingly, the performance of the ICI compensation with no IUI removal is outperformed by the CPE compensation with IUI removal method in the case where the channel effect was added to the simulation. The proposed technique therefore manages to provide a gain as expected.

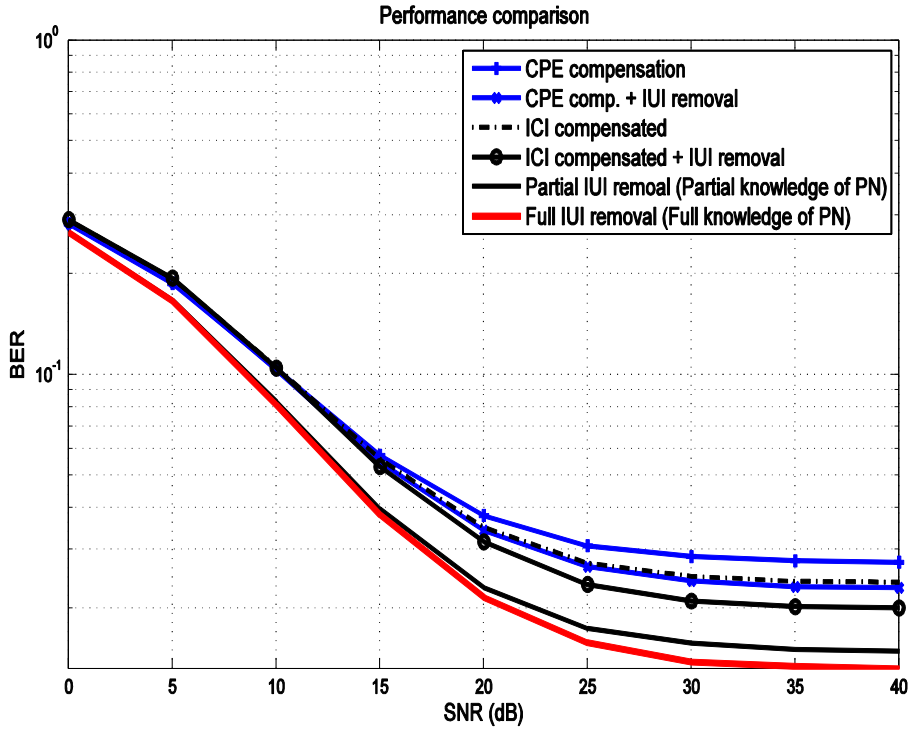

Figure 5.3 *- BER vs. SNR plot for different phase noise mitigation methodologies (Extended ITU-R Vehicular A channel, 50 Hz phase noise 3-dB bandwidth, SNR=20 dB.*

Figure 5.4 shows the relationship between the BER of the middle user and the applied phase noise bandwidth of the edge users. The phase noise applied to the middle

user was fixed to 50 Hz while the phase noise of the edge users was equally increased starting from the 3-dB phase noise bandwidth value of 1 Hz and ending with 500 Hz. The middle user's SNR was fixed through the whole simulation to 20 dB. As it was expected, as the 3-dB bandwidth of the edge users increases, the IUI increases and degrades the BER of the middle user. Additionally, it can be noticed that at low edge user's 3-dB bandwidth (1 until 10 Hz), the difference between phase noise compensation methods with and without IUI removal is insignificant and at high edge user's 3-dB bandwidth (500 Hz), all practical phase noise mitigation methods perform almost similarly with poor BER values. Furthermore, the CPE mitigation which involves the IUI removal method even outperforms the conventional ICI mitigation method when the phase noise 3-dB bandwidth of the edge users is more than 100 Hz.

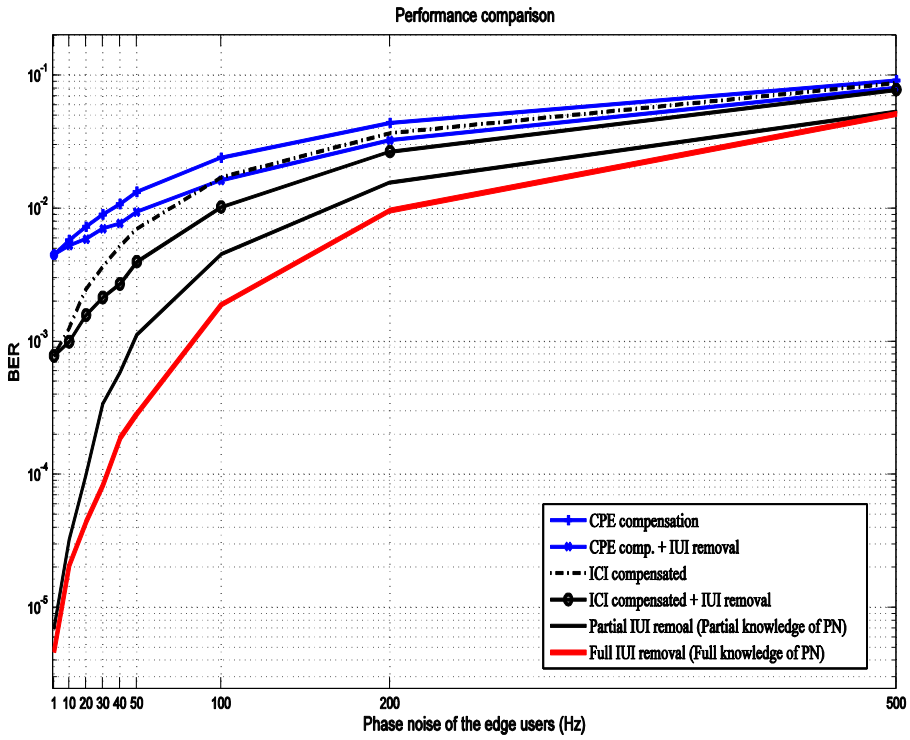

Figure 5.4 *- BER vs. edge users phase noise bandwidth (AWGN channel). The middle users phase noise 3-dB bandwidth was fixed to 50 Hz and the power difference between the edge users and the middle one was fixed to 10 dB, SNR=20 dB.*

Figure 5.5 depicts the same scenario that was described in Figure 5.4. The only difference is that the OFDMA waveform experiences the ITU-R Vehicular A multipath channel model. The overall system performance is deteriorated when compared with the case where the signal goes through an AWGN channel. In this case, the phase noise 3-

dB bandwidth of the edge users where the CPE mitigation involving the IUI removal method outperforms the conventional ICI mitigation method is slightly less than 50 Hz.

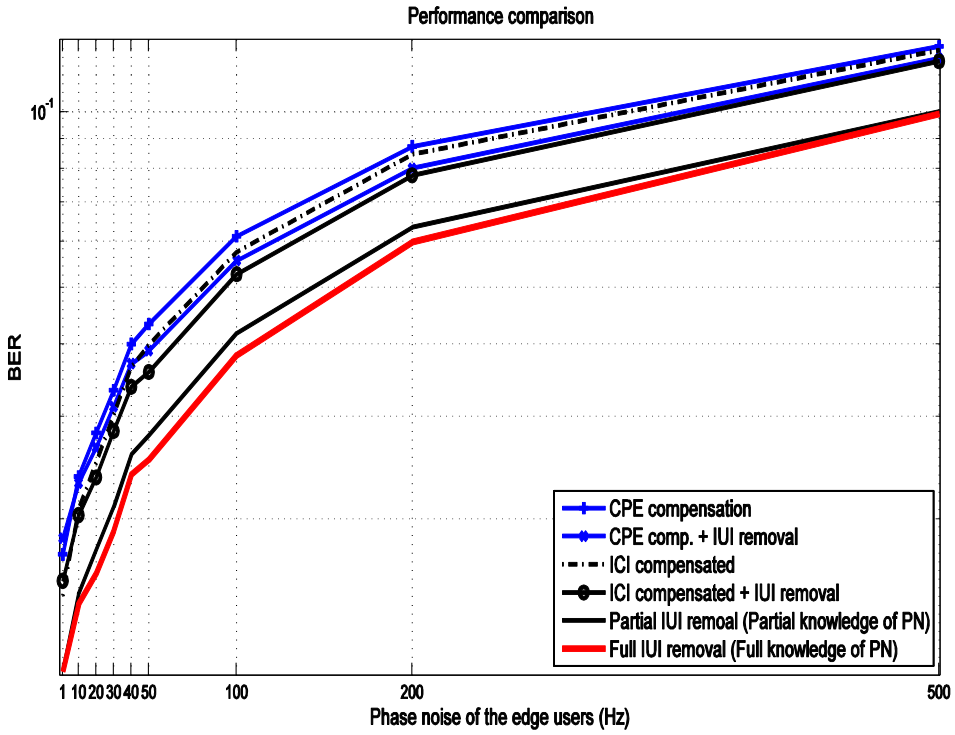

Figure 5.5 *- BER vs. edge users phase noise bandwidth (ITU-R Vehicular A channel). The middle users phase noise 3-dB bandwidth was fixed to 50 Hz and the power difference between the edge users and the middle one was fixed to 10 dB, SNR=20 dB.*

Figure 5.6 shows the relationship between the BER and the power difference between the middle and the edge users. This simulation scenario represents a part of the problem in this study that causes the spread over the middle user. As expected, the performance of the OFDMA transceiver for the middle user in this simulation degrades as the power difference between the edge users and the middle one increase. At low power difference between the middle and edge users (0 until 3dB), the phase noise estimation techniques with and without IUI removal have close performance, and the difference starts to be noticed after around 6 dB. Additionally, at high power difference (more than 20 dB), all practical mitigation methods result in a relatively similar and poor BER performance.

It can be noticed from the figure that the CPE mitigation technique with IUI removal outperforms the conventional ICI mitigation technique after around 12 dB of power difference.

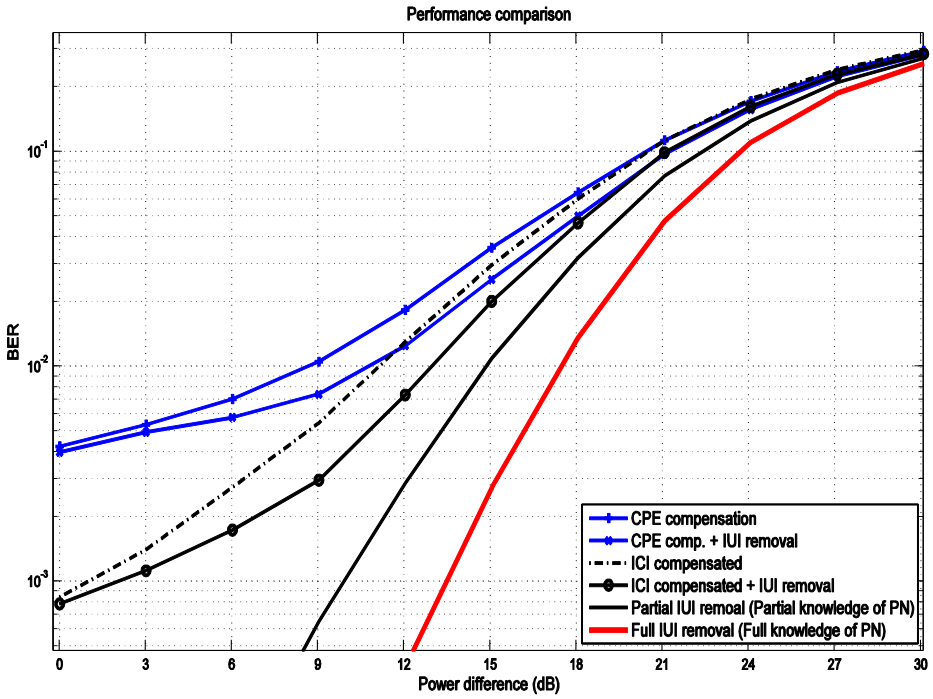

Figure 5.6 *- BER vs. the power difference between the edge users and the middle users (AWGN channel). The 3-dB phase noise bandwidth was fixed to 50 Hz for all users, SNR=20 dB.*

In Figure 5.7, the ITU-R Vehicular A channel was added in the simulation. When the channel effect was added, the CPE mitigation technique with IUI removal outperforms the conventional ICI mitigation technique in this case at around 8 dB of power difference between the middle and edge users.

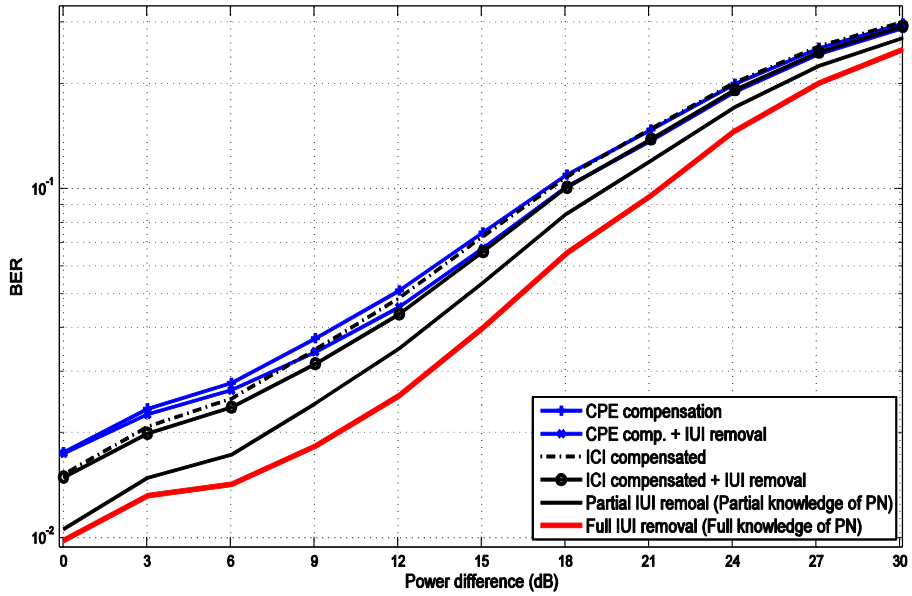

Figure 5.7 *- BER vs. the power difference between the edge users and the middle users (ITU-R Vehicular A channel). The 3-dB phase noise bandwidth was fixed to 50 Hz for all users, SNR=20 dB.*

6. CONCLUSION

In this thesis, a theoretical overview of the OFDM multicarrier modulation technique and OFDMA and its implementations in various wireless communications standards was made. A specific drawback in OFDM, oscillator phase noise, was studied and its effect in OFDMA systems was deduced. Subsequently, a proposed method to mitigate the phase noise induced IUI in OFDMA was applied in simulations. The method had shown to provide a gain when applied. The gain was recognized when the application of phase noise spread estimation and mitigation techniques outperformed the conventional CPE and ICI estimation and mitigation methods that did not take into account the phase noise induced spread from adjacent users.

Since the method proved to provide a gain, the next step is to provide a more robust channel estimation technique to estimate the channel's response beyond a user's band. This can be achieved by inserting pilot data beyond a user's allocated bandwidth in the bandwidth allocated to the adjacent user. This suggestion is of importance when the phase noise induced spread estimation is to be performed far beyond a user's band edges.

An interesting implementation of the IUI mitigation technique is when it is applied for a different scenario where the subcarrier assignment in an OFDMA symbol is not contiguous but distributed. In a random subcarrier assignment in an OFDMA symbol, the pilots are distributed along the whole OFDMA symbol bandwidth and not solely restricted to a user's defined band as in the case of the contiguous subcarriers assignment. This realization is of great benefit since a user's channel can be estimated along the whole OFDMA symbol.

References:

[1] ‘3rd Generation Partnership Project; Technical Specification Group Radio Access Network; Evolved Universal Terrestrial Radio Access (E-UTRA); User Equipment (UE) radio transmission and reception (Release 8) ’, 3GPP, 3GPP TR 45.912.
[2] ‘3rd Generation Partnership Project; Technical Specification Group Radio Access Network; Requirements for Evolved UTRA (E-UTRA) and Evolved UTRAN (E-UTRAN) (Release 7)’, 3GPP, 3GPP TR 45.912.

[3] J. Bhatti, M. Moeneclaey, “Iterative soft-decision-directed phase noise estimation from a DCT basis expansion,” in *Proc. International Symposium on Personal, Indoor and Mobile Radio Communications* (*PIMRC’09*), Tokyo, Japan, September 2009, pp.3228-3232.
[4] J. Bhatti, N. Noels, and M. Moeneclaey, “Algorithms for iterative phase noise estimation based on a truncated DCT expansion,” in *Proc. International Workshop on Signal Processing Advances in Wireless Communications* (*SPAWC’11*), San Francisco, CA, June 2011, pp. 51-55.
[5] J. Bhatti, N. Noels, and M. Moeneclaey, “Phase noise estimation and compensation for OFDM systems: a DCT-based approach,” in *Proc. International Symposium on Spread Spectrum Techniques and Applications 2010*, Taichung, Taiwan, October 2010, pp. 93-97.
[6] S. Bittner, A. Frotzscher, G. Fettweis, and E. Deng, “Oscillator phase noise compensation using Kalman tracking,” in *Proc. International Conference on Acoustics, Speech and Signal Processing 2009* (*ICASSP’09*), Taipei, Taiwan, April 2009, pp. 2529-2532.
[7] S. Bittner, W. Rave, and G. Fettweis, “Joint iterative transmitter and receiver phase noise correction using soft information,” in *Proc. IEEE International Conference on Communications 2007* (*ICC’07*), Glasgow, Scotland, June 2007, pp. 2847-2852.
[8] S. Bittner, E. Zimmermann, and G. Fettweis, “Exploiting phase noise properties in the design of MIMO-OFDM receivers,” in *Proc. IEEE Wireless Communications and Networking Conference 2008* (*WCNC’08*), Las Vegas, NV, March 2008, pp. 940-945.
[9] S. Bittner, E. Zimmermann, and G. Fettweis, “Iterative phase noise mitigation in MIMO-OFDM systems with pilot aided channel estimation,” in *Proc. Vehicular Technology Conference 2007 Fall* (*VTC’07-Fall*), Baltimore, MD, September 2007, pp. 1087-1091.

[10] R. Casas, S. Biracree, and A. Youtz, “Time domain phase noise correction for OFDM signals,” *IEEE Transactions on Broadcasting*, Vol. 48, No. 3 , pp. 230-236, September 2002.

[11] Chuang, J., and N. Sollenberger, " Beyond 3G: Wideband wireless data access based on OFDM and dynamic packet assignment ," *IEEE Personal Comm. Mag.*, vol. 38, no. 7, pp. 78-87, July 2000.

[12] E. Costa, S. Pupolin, “M-QAM-OFDM System Performance in the Presence of a Nonlinear Amplifier and Phase Noise,” *International Journal on Computer Science and Engineering*, Vol. 50, No. 03, 2002.

[13] Erik Parkvall Dahlman, Johan Stefan Skold, *3G Evolution : Radio Access for Mobile Broadband*, Kidlington, GBR: Academic Press, 07/2007.

[14] ‘Digital Video Broadcasting (DVB); Framing structure, channel coding and modulation for digital terrestrial television ’, ETSI EN 300 744, V1.6.1 (2009-01).

[15] A. Goldsmith, *Wireless Communication*, Cambridge University Press, 2005, 672 p., ISBN 978-0521837163.

[16] ‘Introduction to 802.11ac WLAN Technology and Testing’, Agilent Technologies, 2012.

[17] LTE Encyclopedia. Retrieved August 4, 2013, from https://sites.google.com/site/lteencyclopedia/home

[18] P. Mörters and Y. Peres, Brownian Motion, Cambridge University Press, 2010, ISBN 978-0521760188.

[19] “Official IEEE 802.11 working group project timeline”. September 2009, Retrieved in 5-08-2013.

[20] Ramjee Parsad, Shinsuke Hara, *Multicarrier Techniques for 4G Mobile Communications*, Norwood, MA, USA: Artech House, May 2003.

[21] Ramjee Jha Parsad, Uma Shankar, *OFDM Towards Fixed and Mobile Broadband Wireless Access, Morwood*, MA, USA: Artech House, 2007.

[22] D. Petrovic, W. Rave, and G. Fettweis, “Effect of phase noise on OFDM systems with and without PLL: Characterization and compensation,” *IEEE Transactions Communications*, Vol. 55, No. 8, pp. 1607-1616, August 2007.

[23] P. Rabiei, W. Namgoong, N. Al-Dhahir, "On the Performance of OFDM-Based Amplify-and-Forward Relay Networks in the Presence of Phase Noise, " in Proc. *IEEE Transactions on Communications*, vol. 59, no. 5, pp. 1458-1466, May 2011.

[24] P. Robertson and S. Kaiser, "Analysis of the effects of phase noise in orthogonal frequency division multiplex (OFDM) systems," in *Proc. IEEE International Conference on Communications 1995* (*ICC'95*), Seattle, WA, June 1995, pp. 1652-1657, Vol. 3.

[25] R. Sharma, G. Singh, R. Agnihotri, "Comparison of performance analysis of 802.11a, 802.11b and 802.11g standard*," International Journal on Computer Science and Engineering*, Vol. 02, No. 06, 2010.

[26] V. Syrjälä, *Analysis and Mitigation of Oscillator Impairments in Modern Receiver Architectures*, Tampere University of Technology Library, ISSN 1459-2045, April 2012.

[27] V. Syrjälä and M. Valkama, "Analysis and mitigation of phase noise and sampling jitter in OFDM radio receivers," *International Journal of Microwave and Wireless Technologies*, Vol. 2, No. 2, April 2010.

[28] V. Syrjälä and M. Valkama, "Flexible Adjacent Channel Interference and Phase Noise Suppression in Energy-Efficient OFDMA Receivers," *In Proc. IEEE International Workshop on Computer-Aided Modeling Analysis and Design of Communication Links and Networks 2012, CAMAD'12*, Barcelona, Spain, September 2012.

[29] V. Syrjälä and M. Valkama, "Iterative receiver signal processing for joint mitigation of transmitter and receiver phase noise in OFDM-based cognitive radio link", in *Proc. International Conference on Cognitive Radio Oriented Wireless Networks 2012, CROWNCOM'12*, Stockholm, Sweden, June 2012.

[30] V. Syrjälä and M. Valkama, "Receiver DSP for OFDM systems impaired by transmitter and receiver phase noise," in *Proc. IEEE International Conference on Communications 2011, IEEE ICC 11*, Kyoto, Japan, June 2011.

[31] V. Syrjälä, M. Valkama, N. N. Tchamov, and J. Rinne, "Phase noise modelling and mitigation techniques in OFDM communications systems," in *Proc. Wireless Telecommunications Symposium 2009* (*WTS'09*), IEEE, Prague, Czech Republic, April 2009.

[32] N. N. Tchamov, J. Rinne, A. Hazmi, M. Valkama, V. Syrjälä, and M. Renfors, "Enhanced algorithm for digital mitigation of ICI due to phase noise in OFDM receivers*," IEEE Wireless Communications Letters*, December 2012.

[33] N. Wells, "DVB-T2 in relation to the DVB-x2 Family of Standards", ATSC.

[34] 'Wi-Fi CERTIFIED™ n: Longer-Range, Faster-Throughput, Multimedia-Grade® Networks', Wi-Fi Alliance, 2009.

[35] S. Wu and Y. Bar-Ness, "A phase noise suppression algorithm for OFDM-based WLANs," *IEEE Communications Letters*, Vol. 6, No. 12, pp. 535-537, December 2002.

[36] Yang, Samuel C. , *OFDMA System Analysis and Design*, Norwood, MA, USA: Artech House, August 2010.